Table 2
Growth rate of MAC in 7H9 broth.

Strain	Ratio of CFUs at[a]		
	Day 1	Day 3	Day 5
33	0.91 ± 0.28	38 ± 0.86	63 ± 10
198	0.93 ± 0.17	12 ± 1.9	18 ± 4.0
288	0.85 ± 0.20	4.3 ± 1.9	16 ± 0.95
27	1.1 ± 0.25	7.3 ± 2.2	120 ± 21
36	0.83 ± 0.093	5.4 ± 0.21	11.0 ± 1.7
347	0.96 ± 0.16	2.7 ± 1.1	44 ± 19
25291	1.6 ± 0.25	4.8 ± 0.24	110 ± 16*
35767	0.97 ± 0.12	11 ± 3.0	370 ± 43**

* Significantly different ($P < 0.005$) from values for strain 198, 288, and 36 as calculated by Scheffé's test.
** Significantly different ($P < 0.0001$) from values for all clinical strains as calculated by Scheffé's test.
[a] Means ± standard deviations of the ratio of CFUs to those at day 0.

the growth rate among these strains except strain 198 during infection.

On light microscopic observation, THP-1 cell morphologies were not different between infected and uninfected cells (data not shown). We then assessed cytotoxicity by the levels of lactate dehydrogenase (LDH) released into the culture supernatants at day 7. The LDH release was detectable in strain 33 and the laboratory strains (strain 33; 5.8 ± 1.5%, ATCC 25291; 11 ± 1.0%, ATCC 35767; 12 ± 1.9%, without significant difference among these strains); however, it was not detectable in other clinical isolates.

2.4. Pathogenesis of clinical isolates in mice

Female C57BL/6 mice were infected by intratracheal instillation with each strain. Bacterial load in lungs, livers, and spleens were evaluated, and histological inflammation was visually analyzed in 5-mice per strain at defined time points during 16 weeks of infection. There was no significant difference in lung CFUs among strains tested 1 day after the inoculation.

Strain 198 showed high bacterial load, and tended to increase gradually both in lungs and spleens during 16 weeks of infection ($P = 0.08$ between day 1 and 16 weeks) (Fig. 1). Strain 198 was loaded in lungs significantly higher than strain 27 ($P = 0.04$) and 33 ($P = 0.0006$) at 8 weeks of infection, and than strain 33 ($P = 0.0009$), 288 ($P = 0.001$), 36 ($P = 0.0003$), and 347 ($P = 0.004$) at 16 weeks. Histologically, strain 198 induced strong inflammation in lungs, which was paralleled with bacterial loads (Fig. 2). ATCC 25291, known as highly a virulent strain in mice [12], showed initial reduction of bacterial load in lungs at 4 weeks of infection ($P = 0.01$ between day 1 and 4 weeks) and rapid increase in bacterial load in lungs after 4 weeks of infection. ATCC 25291 was comparatively virulent to strain 198 with respect to the high bacterial load in lungs and spleens, and severe pulmonary inflammation at 16 weeks of infection. By contrast, other clinical isolates did not increase profoundly in lung CFUs; however, these strains were never eliminated from lungs. ATCC 35767 was rapidly decreased and undetectable in lungs, spleens and livers within 16 weeks of infection. Overall, the clinical isolates other than strain 198 exhibited limited histological lesions with transient inflammatory changes in lungs 4 weeks after the inoculation, and thereafter the inflammation subsided at 16 weeks.

Table 3
Growth rate of MAC in THP-1 cells.

strain	Ratio of CFUs at[a]	
	Day 2	Day 7
33	0.29 ± 0.12	0.25 ± 0.16
198	18 ± 12*	1.30 ± 0.68*
288	0.47 ± 0.26	0.097 ± 0.055
27	0.54 ± 0.37	0.28 ± 0.11
36	2.4 ± 1.2	0.31 ± 0.11
347	1.1 ± 0.49	0.36 ± 0.23
25291	0.16 ± 0.048	0.11 ± 0.038
35767	0.059 ± 0.029	0.0070 ± 0.0048

* Significantly different ($P < 0.0001$) from values for any other strains studied as calculated by Scheffé's test.
[a] Means ± standard deviations of the ratio of CFUs to those at day 0.

3. Discussion

Virulence is defined as the quantitative ability of an agent to cause disease. The virulence of mycobacteria can be evaluated by the infection to macrophages and animals [17]. This is the first study that examined the virulence of MAC isolates from immunocompetent patients with different types of disease outcome. We found that strain 198, which derived from a patient with most serious disease, revealed high bacterial load both in THP-1 cells and in C57BL/6 mice among isolates studied. Strain-specific virulence of MAC has been implicated by some previous studies of the serovar 4 *M. avium* isolated from patients. In AIDS-related MAC disease, a serovar 4 *M. avium* isolate has shown to be one of the frequently isolated type [13], and a previous analysis of a serovar 4 isolate and ATCC strain has shown the superior virulence of serovar 4 *M. avium* in human macrophages [14]. In non-AIDS pulmonary MAC disease, our recent prospective study indicates that patients infected with serovar 4 *M. avium* has poorer prognosis than those infected with MAC of other serovars [16]; however, to our best knowledge, no study has shown the direct data of mycobacterial virulence of clinical isolates and clinical disease outcome. Strain 198 is the first MAC isolate whose experimental virulence corresponds to the serious disease outcome in humans. Thus, strain 198 has strain-specific strong virulence for immunocompetent humans and mice. We consider that strain 198 is worth further genetic investigation of virulence factors.

MAC strains hypervirulent for mice has been isolated previously by Pedrosa et al. including ATCC 25291 and MAC 101, which proliferate profoundly in mouse macrophages and in mice *in vivo* [12]. In this study, strain 198 proliferated in human macrophages, in correspondence with rapid clinical disease progression and additionally in mouse lungs. The consistency between experimental virulence in human cells and clinical disease outcome suggests that the capability of inducing such strong pathogenesis may be attributed mostly to the characteristics of the pathogen, i.e. virulence factor(s) for mammalian cells unique to strain 198. Previously Birkness et al. has shown the strong cytotoxic effect and growth of serovar 4 *M. avium* isolated from an AIDS patient in blood mononuclear cell-derived human macrophages compared with a serovar 2 strain from chickens (ATCC 35713). Therefore, we evaluated cytotoxicity of MAC strains by the microscopic morphology and by the LDH release from infected THP-1 cells; however, contrary to the expectation, strain 198 was not cytotoxic to THP-1. In addition, the release of LDH was lower in strain 33, ATCC 25291, and ATCC 35767 than in the previous experiment of *M. tuberculosis* infection to THP-1 cells (cytotoxicity in cases of *M. tuberculosis* H37Rv and H37Ra; approximately 30%) [18]. We assume that cytotoxic effect may not play a major role in displaying the virulence of MAC during infection, suggested by the similar result by Huttunen et al. showing the lack of cytotoxic effect of MAC in human 28SC macrophage and A549 lung epithelial cell lines evaluated by 3-(4,5-dimethyl-2-thiazolyl)-2,5-diphenyl-2H tetrazolium bromide (MTT) assay [19]. We speculate the virulence of strain 198 depends on the ability to survive or proliferate in macrophages rather than cytotoxic effect, which, may be causative for severe pulmonary MAC disease with rapid disease progression within a few years.

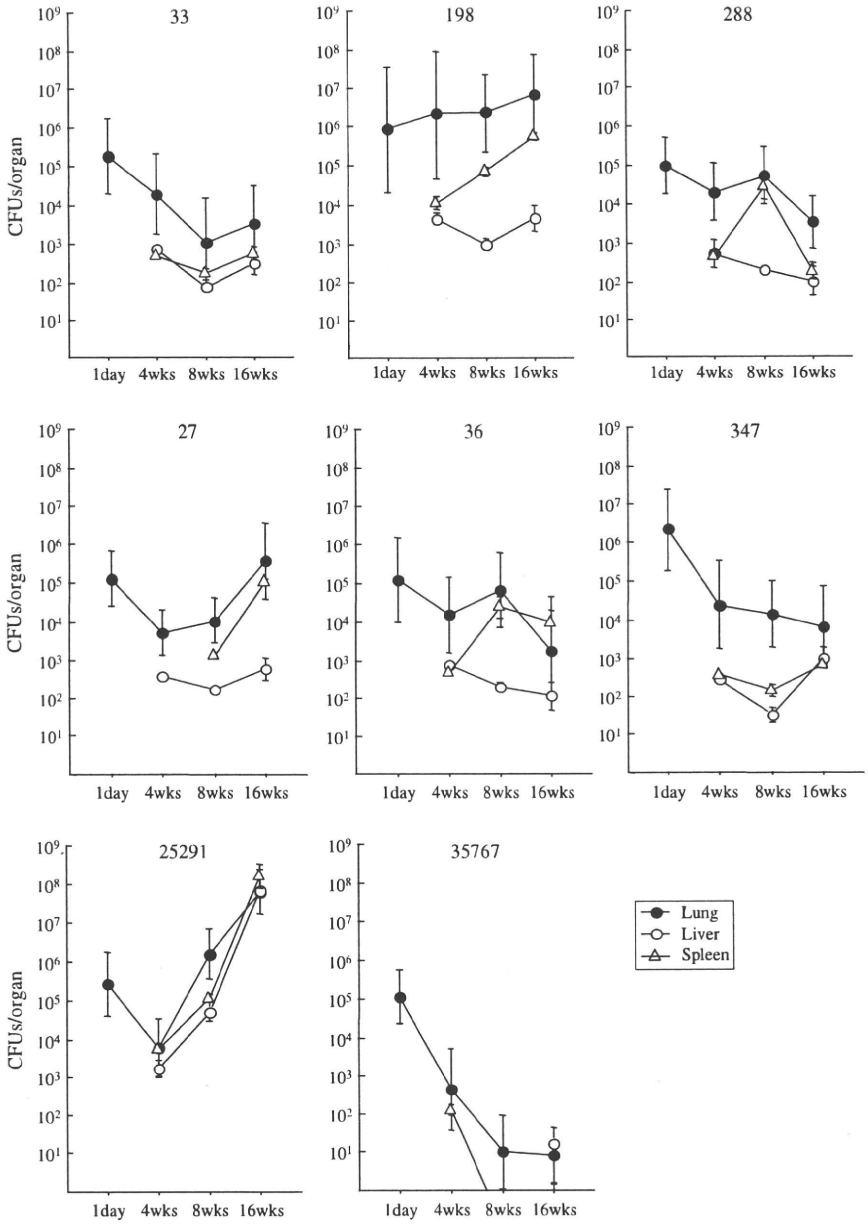

Fig. 1. Time course of mycobacterial growth in lungs, spleens and livers of C57BL/6 mice. Bacterial suspensions containing 1×10^5 CFUs were inoculated intratracheally to female C57BL/6 mice at the age of 7 weeks ($n = 20$ per strain). The lungs, livers and spleens of 5 mice per strain were sectioned at day 1 (only lungs), 4, 8, and 16 weeks later from challenge Data were presented as means ± standard deviations of CFUs/organ.

In this study, strain 198 showed strong virulence for mice at 16 weeks of infection similar to ATCC 25291; however, virulence for THP-1 cells was quite different, and pathogenic effects for mice within 4 weeks of infection was dissimilar between these two strains. These differences can be explained by the difference of immune response between host species and by the difference of immune phase. First, strain 198 could proliferate, but ATCC 25291 was rapidly eliminated in THP-1 cells (Table 3). In mouse macrophages mycobactericidal activity is attributed to nitric oxide produced by inducible nitric oxide synthase [20], whereas in human macrophages, it is attributed to Toll-like receptor signaling-dependent production of anti-microbial peptides [21,22]. Strain 198 is capable of proliferating under these two patterns of mycobactericidal activities, which suggests that strain 198 may have some virulence factors advantageous to survive both in human and mouse macrophages against mycobactericidal activity of the hosts, in contrast to ATCC 25291 which may lack virulence factors to survive in human macrophages. Second, strain 198 showed high bacterial load in lungs continuingly during 16 weeks of infection in mice, while ATCC 25291 proliferated after initial reduction in lungs at 4 weeks of infection (Fig. 1). The *in vitro* infection model using cell lines and the *in vivo* infection model using mice within 4 weeks reflects early stages of infection; on the other hand, the *in vivo* model after 8 weeks reflects chronic phase of infection [17,23]. The difference of pathogenic effects for mice within 4 weeks of infection suggests that strain 198 may resist both innate and acquired immunity, while ATCC 25291 may resist acquired immunity only. We assume that strain 198 and ATCC 25291 may possess different virulence mechanisms to persist in *in vivo* after development of acquired immunity.

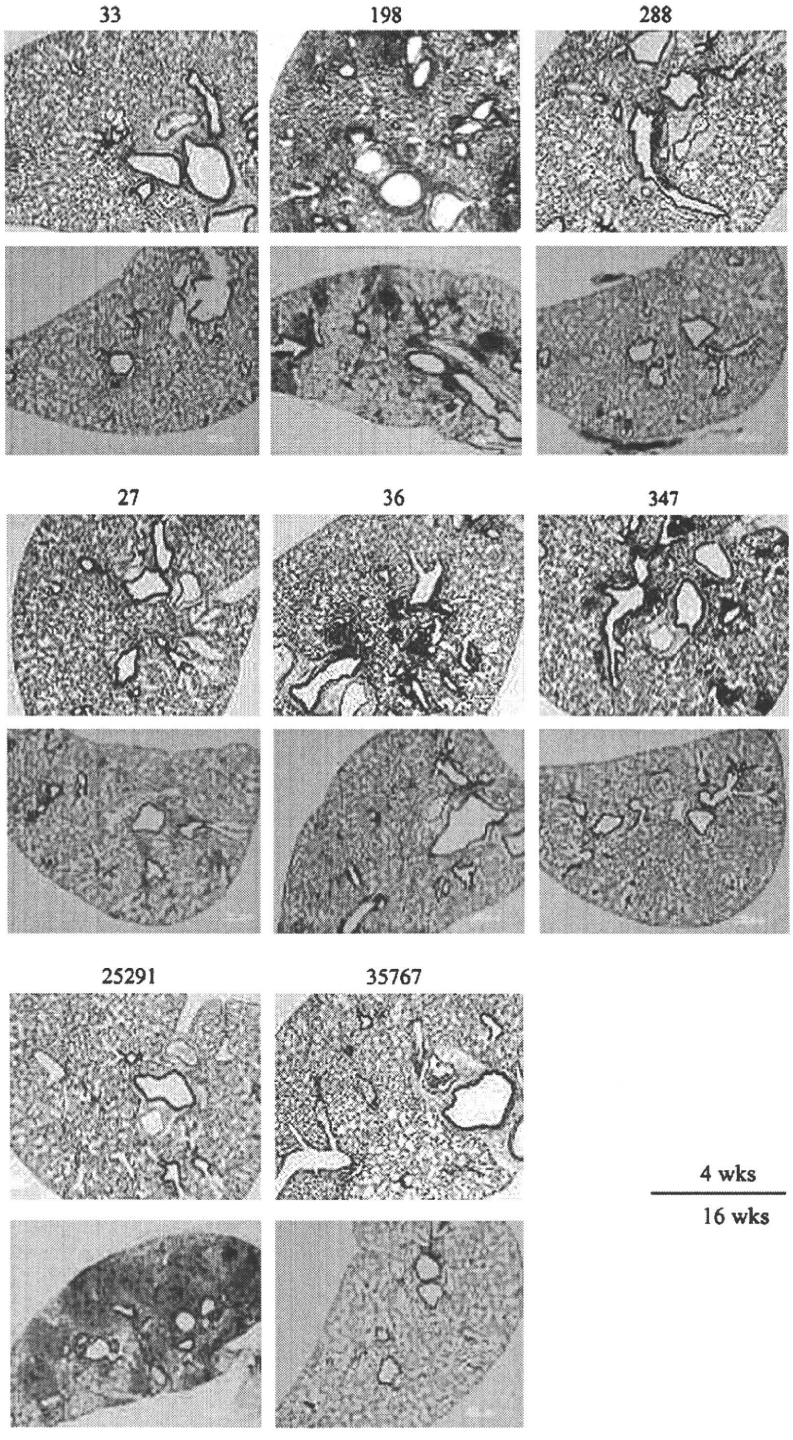

Fig. 2. Histological pictures of the lungs during 4 weeks or 16 weeks of infection in C57BL/6 mice by hematoxylin–eosin staining. Magnification, ×40.

In this study, clinical strains except for strain 198 did not show consistent virulence-associated phenotype among THP-1 cells, C57BL/6 mice, and clinical disease outcome. Similarly, Pedrosa et al. has also revealed that the growth of MAC in bone-marrow derived macrophages does not necessarily predict the virulence in mice by comparing the growth of 41 MAC isolates from various derives including humans, animals, and environment [12]. Although some clinical cases of pulmonary MAC disease may be caused by hypervirulent strains such as strain 198, these findings of clinical and natural isolates suggest that virulence may not the only determinant of the pathogenesis of pulmonary MAC disease in the majority of clinical cases. The development of pulmonary MAC disease depends on the balance between bacterial virulence and host defense. It is widely accepted that patients with pulmonary MAC disease have some characteristics of clinical background, such as males in their 40s and early 50s who have a history of cigarette smoking and excessive alcohol use, and such as postmenopausal, nonsmoking females [3], and these patient characteristics might

possibly indicate unknown predisposing conditions which enhance susceptibility for pulmonary MAC infection. The diverse phenotype of clinical MAC strains may be attributed to the disease susceptibility of the hosts. We propose that pathogenic mechanism of human pulmonary MAC disease include two patterns; one is that the strong virulence of MAC strains such as strain 198 induces rapid mycobacterial growth and serious disease outcome, and the other is that relatively weak to moderate virulence interacts with predisposing conditions of the host, leading the wide range of clinical outcome.

This study was preliminary in that we did not identify the mechanism of hypervirulence of strain 198. We observed the consistency between hypervirulence in human macrophages bedsides in immunocompetent mice and severe clinical outcome only in strain 198, not in any other isolates studied. From this finding, we speculate the existence of strain-specific virulence factors of strain 198. Recent exponential advances have enabled whole genome sequence of two *M. avium* strains, *M. avium* 104 and *M. avium* subsp. *paratuberculosis* K-10. Based on these exhaustive information, comparative genomics of MAC organisms has revealed the different genomic components regarding virulence factors, such as *ser2* encoding glycosylation enzyme of the lipopeptide core to generate the glycopeptidolipids, mammalian cell entry (*mce*) gene homologs, and PE/PPE genes (i.e., with Pro Glu and Pro Pro Glu motifs) [24]. In addition, there are large sequence polymorphisms among MAC organisms, suggesting a large corresponding diversity in virulence [11,24]. We speculate that the virulence of MAC strains including strain 198 may be determined by insertion or deletion of virulence genes encoding known [24] or unknown virulence factors.

In summary, we demonstrated that certain clinical strain derived from patients of the progressive pulmonary MAC disease exhibits strong virulence in human macrophages and in immunocompetent mice. Among clinical isolates, strain 198 is the first isolate hypervirulent to both human macrophages and mice. Our data suggest that strain-to-strain differences in virulence may play a significant role in disease progression in humans. Although Sarmento et al. showed that capability of TNF-α production from macrophages inversely correlates with the virulence of MAC strains [25], we could not find such relationship among the isolates (data not shown). In future studies, we will identify the virulence/pathogenicity-associated factor(s) of strain 198 and survey the frequency of strain variation in immunocompetent patients with pulmonary MAC disease.

4. Materials and methods

4.1. Bacterial strains

We used six clinical isolates from non-AIDS patients with pulmonary MAC disease and two laboratory strains, *M. avium* ATCC 25291 (serovar 2) and *M. avium* ATCC 35767 (serovar 4), in this study. Clinical isolates were obtained between September and November in 2003 at Toneyama National Hospital. Informed consent was obtained from all patients according to the guideline of Institutional Review Board of Toneyama National Hospital. Diagnosis of pulmonary MAC disease was made according to the American Thoracic Society guideline [3]. The samples were derived from two groups of patients; one group exhibited progressive disease in spite of the combination chemotherapy including clarithromycin, ethambutol and rifampin recommended by the American Thoracic Society guideline (progressive type) [3], the other displayed no exacerbation without anti-microbial chemotherapy for approximately ten years or more (silent type). These types were determined by the laboratory findings at the period of sputum sampling (including sputum smear and culture, chest X-ray findings, and erythrocyte sedimentation rate) and the rapidness of disease progression (Table 1). Sputum specimens were mixed with 2% sodium hydroxide, and *N*-acetyl-L-cysteine and then centrifuged for 15 min at 3000 *g*. The supernatants were discarded, and the sediment was mixed at 1:10 (vol/vol) with sterile water. The bacteria were cultivated in Middlebrook 7H9 broth supplemented with albumin–dextrose–catalase, 0.02% glycerin and 0.05% Tween 80, and then kept at −80 °C until following experiments. Identification of MAC was made by polymerase chain reaction using a commercially available kit (AMPLICOR Mycobacterium Tuberculosis Test, Roche, Basel, Switzerland). The serovars of clinical isolates were identified by the liquid chromatography/mass spectrometry as described previously [26]. Strains not containing serovar-specific oligosaccharides were defined as apolar type.

4.2. Growth in 7H9 broth

Bacterial suspension was adjusted to be 0.2 by optical density (OD) at 630 nm. The samples were cultured in 5 ml of 7H9 media in plastic tubes without agitation After vortexing to dissolve aggregates, cultivated bacterial suspensions were inoculated at days 1, 3, and 5 by serial 10-fold dilutions on Middlebrook 7H11 agar plates supplemented with oleic acid–albumin–dextrose–catalase, and 0.05% glycerol (7H11-OADC) agar plates in triplicate. The number of CFUs was counted after cultivating at 37 °C for 3 weeks.

4.3. Infection of THP-1 cells with MAC in vitro

THP-1 cells were purchased from Health Science Research Resources Bank (Tokyo, Japan). The cells were cultured in RPMI1640 containing 10% heat-inactivated fetal bovine serum (FBS; Equitech-bio, TX), and subcultured every 3–4 days. THP-1 cells were differentiated by 100 nM PMA (Sigma–Aldrich, St Louis, MO) for 48 h before infection. Before 48 h of infection, 1 ml of 2×10^5/ml cells was cultured in RPMI1640 containing 5% human serum (AB-blood group) in 24-well plates. Then, 1 ml of 2×10^4 CFUs/ml bacteria was exposed to the cultured cells for 24 h without opsonization (multiplicity of infection; 0.1 bacteria/cell). After that, the cells were treated with 20 μg/ml of gentamicin for 3 h to kill extracellular bacteria, followed by washing 4 times by RPMI1640. The infected cells were cultured in 2 ml of RPMI1640 containing 5% human serum. At days 0 and 7, uninfected bacteria were removed by washing with RPMI1640 4 times, and 500 μl of filter-sterilized phosphate buffered saline containing 0.5% Triton X-100 (Wako, Osaka, Japan) was treated per well to lyse cell membrane. The intracellular survival of bacteria was determined by counting CFUs by inoculating the cell lysate on 7H11-OADC agar plates. The experiment was performed in triplicate.

4.4. Assays for cytotoxicity

Cytotoxic effects were evaluated by the release of LDH from the cells. LDH activity of culture supernatants was determined by a commercially available kit (Roche, Basel, Switzerland). Supernatants were diluted to be 10^{-1} by distilled water for optimal reaction. The diluents were reacted with reaction mixture for 30 min, and then the OD was measured at 492 nm. Supernatants of completely lysed uninfected cells with filter-sterilized phosphate buffered saline containing 20% Triton X-100 and those of uninfected cells untreated with Triton X-100 were served as high and low controls, respectively. Cytotoxicity (%) was calculated as follows; $(OD_{sample} - OD_{low\ control}) \times 100/(OD_{high\ control} - OD_{low\ control})$. The measurement was performed in triplicate.

4.5. Animal studies

Female C57BL/6 mice aged at 6 weeks were purchased from CLEA Japan (Tokyo, Japan). All mice were kept under specific pathogen free conditions in animal facility of Osaka City University Graduate School of Medicine according to the institutional guidelines for the animal experiments. Twenty mice were used per group for infecting with each strain. One hundred microlitre of bacterial suspension containing 1×10^5 CFUs of MAC was inoculated into the trachea of the 7 weeks-aged mice anesthetized with pentobarbital sodium. Lungs, spleens and livers were removed on day 1 (only lungs) and 4, 8, 16 weeks after inoculation from 5-mice per strain. The organs were homogenized in 1 ml saline, and 0.1 ml of 10-fold dilutions of the homogenates was plated on 7H11-OADC agar followed by cultivating for 3 weeks. Bacterial burden was evaluated by CFUs per organ. Histological sections were made by standard methods including formalin fixation, dehydration, embedding in paraffin, and staining with hematoxylin and eosin.

4.6. Statistical analysis

Data were analyzed using the statistical analysis software package StatView 5.0 (SAS Institute, Cary, NC). The difference of mycobacterial growth in 7H9 broth, THP-1 cells, and mice was compared by a post hoc test of Scheffé among the strains tested. The difference of mycobacterial growth at defined time points during infection in THP-1 cells as well as in mice was compared by repeated measurement ANOVA with a post hoc test of Scheffé in the individual strains. Difference was considered statistically significant at $P < 0.05$.

Acknowledgement

We thank Todd P. Primm for the critical comments on the manuscript. We also thank Chihiro Inoue and Sara Matsumoto for the assistance of the experiments and for the heartfelt encouragement. This work was supported by grants from the Ministry of Education, Culture, Sports, Science and Technology, the Ministry of Health, Labour and Welfare (Research on Emerging and Re-emerging Infectious Diseases, Health Sciences Research Grants), The Japan Health Sciences Foundation, and The United States-Japan Cooperative Medical Science Program against Tuberculosis and Leprosy.

References

[1] Horsburgh Jr CR, Gettings J, Alexander LN, Lennox JL. Disseminated *Mycobacterium avium* complex disease among patients infected with human immunodeficiency virus, 1985–2000. Clin Infect Dis 2001;33:1938–43.
[2] Field SK, Fisher D, Cowie RL. *Mycobacterium avium* complex pulmonary disease in patients without HIV infection. Chest 2004;126:566–81.
[3] Griffith DE, Aksamit T, Brown-Elliott BA, Catanzaro A, Daley C, Gordin F, et al. An official ATS/IDSA statement: diagnosis, treatment, and prevention of nontuberculous mycobacterial diseases. Am J Respir Crit Care Med 2007;175:367–416.
[4] Flynn JL, Goldstein MM, Chan J, Triebold KJ, Pfeffer K, Lowenstein CJ, et al. Tumor necrosis factor-α is required in the protective immune response against *Mycobacterium tuberculosis* in mice. Immunity 1995;2:561–72.
[5] Dorman SE, Picard C, Lammas D, Heyne K, van Dissel JT, Baretto R, et al. Clinical features of dominant and recessive interferon γ receptor 1 deficiencies. Lancet 2004;364:2113–21.
[6] Newport MJ, Huxley CM, Huston S, Hawrylowicz CM, Oostra BA, Williamson R, et al. A mutation in the interferon-γ-receptor gene and susceptibility to mycobacterial infection. N Engl J Med 1996;335:1941–9.
[7] Kampmann B, Hemingway C, Stephens A, Davidson R, Goodsall A, Anderson S, et al. Acquired predisposition to mycobacterial disease due to autoantibodies to IFN-γ. J Clin Invest 2005;115:2480–8.
[8] Patel SY, Ding L, Brown MR, Lantz L, Gay T, Cohen S, et al. Anti-IFN-γ autoantibodies in disseminated nontuberculous mycobacterial infections. J Immunol 2005;175:4769–76.
[9] Roque S, Nobrega C, Appelberg R, Correia-Neves M. IL-10 underlies distinct susceptibility of BALB/c and C57BL/6 mice to *Mycobacterium avium* infection and influences efficacy of antibiotic therapy. J Immunol 2007;178:8028–35.
[10] Ernst JD, Trevejo-Nunez G, Banaiee N. Genomics and the evolution, pathogenesis, and diagnosis of tuberculosis. J Clin Invest 2007;117:1738–45.
[11] Primm TP, Lucero CA, Falkinham 3rd JO. Health impacts of environmental mycobacteria. Clin Microbiol Rev 2004;17:98–106.
[12] Pedrosa J, Florido M, Kunze ZM, Castro AG, Portaels F, McFadden J, et al. Characterization of the virulence of *Mycobacterium avium* complex (MAC) isolates in mice. Clin Exp Immunol 1994;98:210–6.
[13] Hoffner SE, Kallenius G, Petrini B, Brennan PJ, Tsang AY. Serovars of *Mycobacterium avium* complex isolated from patients in Sweden. J Clin Microbiol 1990;28:1105–7.
[14] Birkness KA, Swords WE, Huang PH, White EH, Dezzutti CS, Lal RB, et al. Observed differences in virulence-associated phenotypes between a human clinical isolate and a veterinary isolate of *Mycobacterium avium*. Infect Immun 1999;67:4895–901.
[15] Han XY, Tarrand JJ, Infante R, Jacobson KL, Truong M. Clinical significance and epidemiologic analyses of *Mycobacterium avium* and *Mycobacterium intracellulare* among patients without AIDS. J Clin Microbiol 2005;43:4407–12.
[16] Maekura R, Okuda Y, Hirotani A, Kitada S, Hiraga T, Yoshimura K, et al. Clinical and prognostic importance of serotyping *Mycobacterium avium–Mycobacterium intracellulare* complex isolates in human immunodeficiency virus-negative patients. J Clin Microbiol 2005;43:3150–8.
[17] Smith I. *Mycobacterium tuberculosis* pathogenesis and molecular determinants of virulence. Clin Microbiol Rev 2003;16:463–96.
[18] Danelishvili L, McGarvey J, Li YJ, Bermudez LE. *Mycobacterium tuberculosis* infection causes different levels of apoptosis and necrosis in human macrophages and alveolar epithelial cells. Cell Microbiol 2003;5:649–60.
[19] Huttunen K, Jussila J, Hirvonen MR, Iivanainen E, Katila ML. Comparison of mycobacteria-induced cytotoxicity and inflammatory responses in human and mouse cell lines. Inhal Toxicol 2001;13:977–91.
[20] Chan J, Xing Y, Magliozzo RS, Bloom BR. Killing of virulent *Mycobacterium tuberculosis* by reactive nitrogen intermediates produced by activated murine macrophages. J Exp Med 1992;175:1111–22.
[21] Liu PT, Stenger S, Li H, Wenzel L, Tan BH, Krutzik SR, et al. Toll-like receptor triggering of a vitamin D-mediated human antimicrobial response. Science 2006;311:1770–3.
[22] Thoma-Uszynski S, Stenger S, Takeuchi O, Ochoa MT, Engele M, Sieling PA, et al. Induction of direct antimicrobial activity through mammalian toll-like receptors. Science 2001;291:1544–7.
[23] Abebe F, Mustafa T, Nerland AH, Bjune GA. Cytokine profile during latent and slowly progressive primary tuberculosis: a possible role for interleukin-15 in mediating clinical disease. Clin Exp Immunol 2006;143:180–92.
[24] Turenne CY, Wallace Jr R, Behr MA. *Mycobacterium avium* in the postgenomic era. Clin Microbiol Rev 2007;20:205–29.
[25] Sarmento AM, Appelberg R. Relationship between virulence of *Mycobacterium avium* strains and induction of tumor necrosis factor α production in infected mice and in *in vitro*-cultured mouse macrophages. Infect Immun 1995;63:3759–64.
[26] Nishiuchi Y, Kitada S, Maekura R. Liquid chromatography/mass spectrometry analysis of small-scale glycopeptidolipid preparations to identify serovars of *Mycobacterium avium–intracellulare* complex. J Appl Microbiol 2004;97:738–48.

Biochemical and Biophysical Research Communications 387 (2009) 272–277

Contents lists available at ScienceDirect

Biochemical and Biophysical Research Communications

journal homepage: www.elsevier.com/locate/ybbrc

Dissection of Rab7 localization on *Mycobacterium tuberculosis* phagosome

Shintaro Seto [a], Sohkichi Matsumoto [b], Isamu Ohta [c], Kunio Tsujimura [a], Yukio Koide [a,*,1]

[a] Department of Infectious Diseases, Hamamatsu University School of Medicine, 1-20-1 Handa-yama, Higashi-ku, Hamamatsu 431-3192, Japan
[b] Department of Bacteriology, Osaka City University Graduate School of Medicine, 1-4-3 Asahi-machi, Abeno-ku, Osaka 545-8585, Japan
[c] Research Equipment Center, Hamamatsu University School of Medicine, 1-20-1 Handa-yama, Higashi-ku, Hamamatsu 431-3192, Japan

ARTICLE INFO

Article history:
Received 16 June 2009
Available online 4 July 2009

Keywords:
Macrophage
Mycobacterium tuberculosis
Rab7
Phagosome maturation
Phagolysosome biogenesis

ABSTRACT

The late endosomal marker Rab7 has been long believed to be absent from the phagosome containing *Mycobacterium tuberculosis* (*M.tb*) in macrophage, but the detail kinetics remains elusive. Here, we found that Rab7 is transiently recruited to and subsequently released from *M.tb* phagosomes. For further understanding of the effect of Rab7 dissociation from the phagosome, we examined the localization of lysosomal markers on the phagosome in the macrophage expressing a dominant-negative Rab7. The localization of lysosomal associated membrane protein-2 (LAMP-2) on the phagosome was Rab7-independent, while that of cathepsin D was Rab7-dependent. These results agree with the localization of each lysosomal marker on *M.tb* phagosome at 6 h postinfection-*i.e.*, LAMP-2, but not cathepsin D localized on the majority of *M.tb* phagosomes. These results suggest that the dissociation of Rab7 from *M.tb* phagosome is the important process in inhibition of phagolysosome biogenesis.

Introduction

Engulfment of pathogens by macrophages is an important initial step in the innate immune response. Pathogens phagocytosed by macrophages are enclosed into phagocytic vacuoles and processed by a series of interactions with endosome vesicles. This well-known process is called phagosome maturation. During the maturation process, phagosomes acquire degradative and microbicidal properties and undergo phagolysosome biogenesis by fusing with lysosomes. Several proteins, including Rab GTPase proteins, play pivotal roles in phagosome maturation and phagolysosome biogenesis [1]. Rab5 is associated with early phagosomes followed by recruitment of its effector proteins EEA1 and Class III phosphatidylinositol 3-kinase [2]. Rab7 appears on the phagosome membrane after Rab5 dissociation and resides there during the subsequent phagosome maturation [3]. Rab7 regulates the transportation and fusion of late endosomes and lysosomes [1] and has been implicated in the interaction between phagosomes and late endosomal compartments [4].

Mycobacterium tuberculosis (*M.tb*) is a causative pathogen of tuberculosis and has the ability to survive and proliferate in macrophages by blocking phagolysosome biogenesis [5,6]. In the current model of *M.tb*-induced inhibition of phagolysosome biogenesis, phagosome maturation is arrested at the stage of Rab5-Rab7 conversion [7] on *M.tb* phagosomes, leading to the inhibition of phagolysosome biogenesis [8]. This hypothesis is supported by observations that Rab7 is absent from mycobacterial phagosomes in macrophages [9,10]. However, the model was challenged by an observation that *M.tb* phagosomes are associated with lysosomal markers in the early stage of infection, suggesting that *M.tb* phagosomes fuse with lysosomes [11]. These conflicting observations indicate that more precise studies are necessary, particularly studies focusing on the kinetics of Rab7 localization during *M.tb*-induced inhibition of phagolysosome biogenesis. We therefore investigated the temporal and spatial localization of Rab7 in *M.tb*-infected macrophages, together with that of lysosomal markers, lysosomal associated membrane protein-2 (LAMP-2) and cathepsin D. In this study, we demonstrated that Rab7 is transiently recruited to *M.tb* phagosome, after which *M.tb* promotes the dissociation of Rab7 from the phagosome, suggesting that the dissociation of Rab7 limits the subsequent recruitment of cathepsin D and results in the blocking of phagolysosome biogenesis.

Materials and methods

Cell and bacterial cultures. Raw264.7 macrophage was obtained from the American Type Culture Collection and maintained in Dulbecco's modified Eagle's medium (DMEM; Sigma–Aldrich) supplemented with 10% fetal bovine serum (FBS; Thermo Trace), 25 μg/ml penicillin G, and 25 μg/ml streptomycin at 37 °C under 5% CO_2. *M. tuberculosis* H37Rv was grown to mid-logarithmic phase in 7H9 medium supplemented with 10% Middlebrook ADC (BD Bio-

* Corresponding author. Fax: +81 53 435 2101.
E-mail address: koidelb@hama-med.ac.jp (Y. Koide).
[1] Address: Executive director, Hamamatsu University School of Medicine, 1-20-1 Handa-Yama, Higashi-ku, Hamamatsu 431-3192, Japan

0006-291X/$ - see front matter © 2009 Elsevier Inc. All rights reserved.
doi:10.1016/j.bbrc.2009.06.152

sciences), 0.5% glycerol and 0.05% Tween 80 (*Mycobacterium* complete medium) at 37 °C. *M.tb* transformed with a plasmid encoding DsRed [12] was grown in *Mycobacterium* complete medium containing 25 μg/ml kanamycin. *Staphylococcus aureus* was grown in brain heart infusion broth (BD Biosciences) at 37 °C.

Antibodies. Rabbit anti-Rab7 polyclonal antibody (Sigma–Aldrich), rat anti-mouse LAMP-2 monoclonal antibody (SouthernBiotech), goat anti-mouse cathepsin D polyclonal antibody (R&D systems), rabbit anti-cytochrome C polyclonal antibody (Cell Signaling), mouse anti-GFP monoclonal antibody (TaKaRa Bio) were all purchased. Alexa488- and Alexa546-conjugated anti-IgG antibodies (Invitrogen) and 10-nm gold particle-conjugated anti-mouse IgG antibody (EY Laboratories) were purchased.

Plasmid constructs and transfection. Human Rab7 was amplified by PCR using cDNA derived from HeLa cells as a template and primers CAGATCTATGACCTCTAGGAAGAAAGTGTTGCTG and CGAATTCAGCAACTGCAGCTTTCTGCCG. PCR product of Rab7 was inserted into the pEGFP-C1 (Invitrogen). A constitutive-active and a dominant-negative Rab7 mutant were made by site-directed mutagenesis using the Quick-Change site-directed mutagenesis kit (Stratagene), as previously reported [13]. Three million Raw264.7 cells were transfected with 15 μg of plasmid DNA using an MP-100 electroporator (Digital Bio Technology) according to the manufacturer's instructions. Transfected cells were incubated in DMEM with 10% FBS for 24 h before the start of experiments.

Infection of bacteria. Transfected cells grown on round coverslips in 12-well plates were infected with bacteria. Bacterial cells were washed with PBS containing 0.05% Tween 80 three times and suspended in DMEM with 10% FBS at a multiplicity of infection (MOI) of 10–30. Aliquots of 1 ml of bacterial suspension were added to transfected Raw264.7 cells on coverslips in 12-well plates, followed by centrifugation at 150*g* for 5 min and incubation for 10 min at 37 °C. Infected cells on coverslips were washed with DMEM three times to remove non-infected bacteria, and then incubated with DMEM containing 10% FBS. At the indicated time points, infected cells were fixed with 1% or 3% paraformaldehyde in PBS.

Confocal microscopy. Imaging of cells was performed with a CSU LiveStage LS-1 confocal microscope system (Yokogawa). Four-dimensional (4D) live microscopy was performed with a CSU LiveStage LS-1 confocal microscope system as described previously [14] with modifications. Transfected Raw264.7 cells grown on a 35-mm glass base dish were infected with *M.tb* expressing DsRed. Synchronous infection was performed with centrifugation, washing with DMEM, and incubation with DMEM containing 10% FBS and 20 mM HEPES (pH7.3) without phenol red. Temperature control of the infected cells was carried out by an Onpu-4 incubation system (Taiei-denki). Serial confocal sections (1.5 μm) within a z-stack spanning a total thickness of 20 μm were taken every 5 min from 30 to 155 min after infection. Images with infected bacteria in transfected macrophage cells were chosen from the z-stacks at each time point to make a time-lapse sequence.

Immunoelectron microscopy. M.tb-infected macrophages were fixed with 3% paraformaldehyde and 0.1% glutaraldehyde in PBS overnight at 4 °C. Dehydration was carried out with a series of ethanol washes. Samples were embedded in LR White resin (OKEN) according to the manufacturer's protocol. Thin sections were cut with diamond knives and mounted on nickel grids. The sections were blocked with 3% BSA in PBS for 30 min. Sections were then incubated with anti-GFP antibody (1:30 v/v) in PBS containing 1% BSA overnight at 4 °C, followed by incubation with 10-nm gold-particle-conjugated secondary antibody (1:30 v/v) for 1 h at room temperature. Samples on grids were counter stained with 2% (wt/vol) uranyl acetate and then observed with a JEM-1220 electron microscope (JEOL). Image J was used to quantify the gold particles and the area of phagosomes.

Isolation of microbead and M.tb phagosomes. Six 15-cm plates of Raw264.7 cells were used for each condition. For isolation of the microbead phagosomal fraction, microbeads (2 μm, Polyscience) were added to Raw264.7 cells for 1 h, washed three times with prewarmed DMEM and incubated in DMEM with 10% FBS for the indicated times. Raw264.7 cells were then collected, lysed, and subjected to discontinuous sucrose gradient centrifugation as described previously [4]. For isolation of the *M.tb* phagosomal fraction, bacteria at an MOI of 10–30 were added to Raw264.7 cells in DMEM with 10% FBS for 1 h, washed and then incubated for the indicated times. Infected cells were collected, lysed, and subjected to fractionation as described previously [15]. For immunoblotting analysis, aliquots of 12.5 μg of Raw264.7 cell lysate and 3 μg of phagosomal fraction proteins were separated by SDS–polyacrylamide gel electrophoresis (PAGE) and then subjected to immunoblotting analysis using anti-Rab7 antibody (1:200 v/v), anti-LAMP-2 antibody (1:200 v/v), anti-cathepsin D antibody (1:200), and anti-cytochrome C (1:100 v/v). Band intensities from three independent experiments were quantified by Image J (http://rsb.info.nih.gov/ij/).

Immunofluorescence microscopy. Raw264.7 cells grown on round coverslips in 12-well plates were allowed to phagocytose microbeads or infected with bacteria for the indicated times, fixed with 3% paraformaldehyde in PBS for 1 h at room temperature, permeabilized with 0.1% Triton X-100 in PBS for 5 min, and finally washed with PBS. Fixed cells were blocked with 3% bovine serum albumin in PBS for 1 h followed by staining with the anti-LAMP-2 (1:50 v/v), cathepsin D (1:50 v/v) antibodies for 1 h, and then incubated with Alexa488- or Alexa546-conjugated anti-IgG antibodies (1:1000 v/v) for 1 h.

Statistics. The unpaired two-sided Student's *t*-test was used to assess the statistical significance of differences between the two groups.

Results and discussion

Rab7 transiently localizes on M.tb phagosome

Rab7 has been shown to be absent from mycobacterial phagosomes in macrophages at the time point when its recruitment generally occurs [9,10]. On the other hand, Clemens and Horwitz demonstrated that *M.tb* phagosomes acquired Rab7 in infected HeLa cells [16], and Sun et al. demonstrated the presence of Rab7 on *Mycobacterium bovis* Bacilus Calmette-Guérin phagosomes [17]. However, there are no crucial reports about the interaction between Rab7 and *M.tb* phagosomes in infected macrophages, especially the kinetics of Rab7 localization immediately after infection. We first examined the localization kinetics of Rab7 on the phagosomes in *M.tb*-infected macrophages. For this purpose, Raw264.7 macrophage cell line expressing enhanced GFP fused with Rab7 (EGFP-Rab7) was employed, because no satisfactory staining was obtained with the commercially available anti-Rab7 antibodies. Raw264.7 cells expressing EGFP-Rab7 were infected with *M.tb* expressing DsRed for 30 min or 6 h. Rab7 failed to localize on the majority of *M.tb* phagosomes at 6 h postinfection (Fig. 1B), although clear signals of EGFP-Rab7 was observed on the phagosomes at 30 min postinfection (Fig. 1A). The proportion of Rab7-positive phagosomes containing *M.tb* reached approximately 80% at 30 min postinfection, as observed in macrophages infected with *S. aureus*, and it decreased to about 30% by 6 h (Fig. 1C) and remained at this level until at least 12 h (data not shown). That of *S. aureus* retained more than 80% at 6 and 12 h postinfection (Fig. 1C and data not shown). Rab7 localized on about 75% of heat-inactivated *M.tb* phagosomes at 6 h after phagocytosis (Fig. 1D), suggesting that live *M.tb* actively promotes Rab7 dissociation from the phagosome.

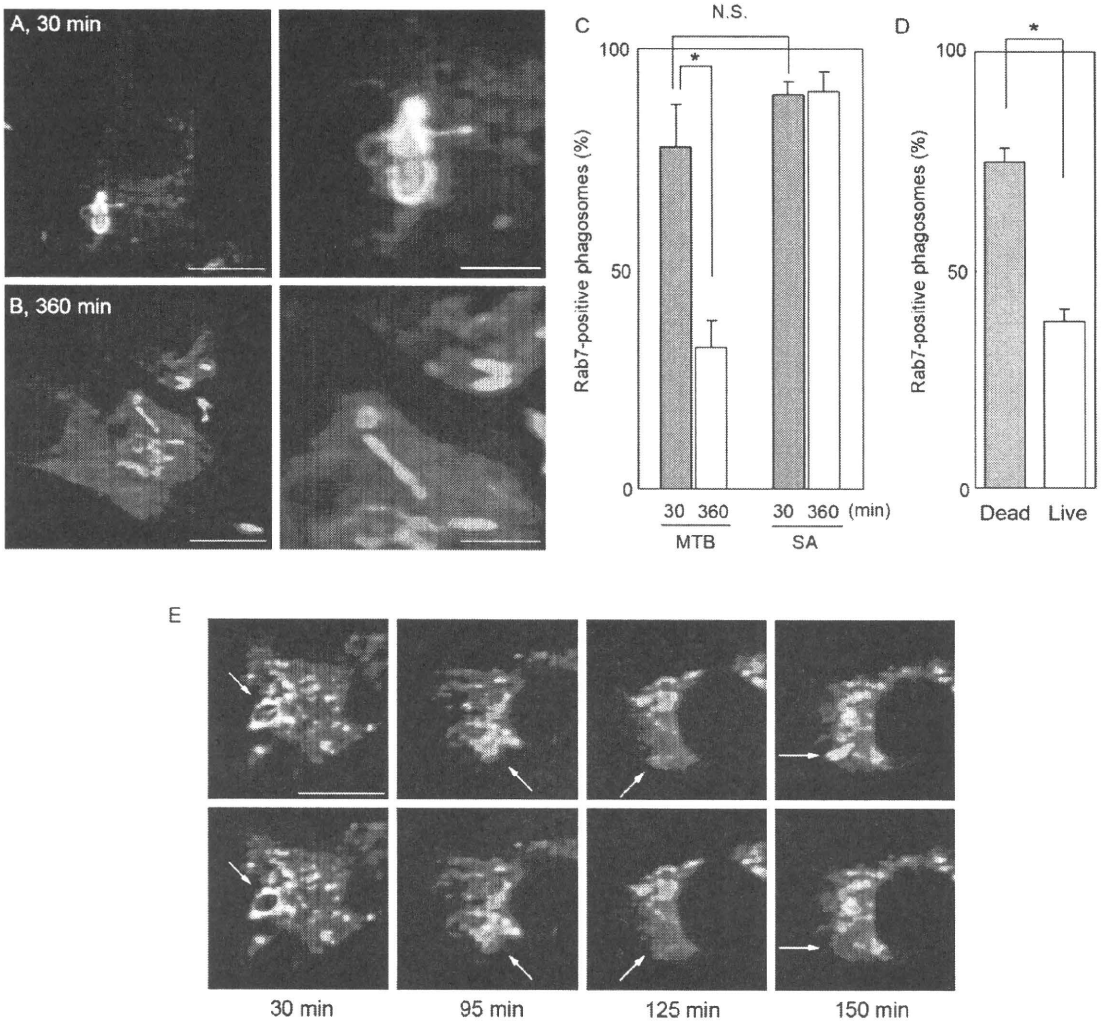

Fig. 1. Dynamics of Rab7 localization on *M.tb* phagosomes. (A, B) Raw264.7 cells expressing EGFP-Rab7 were infected with *M.tb* (MTB) expressing DsRed for 30 min (A) or 6 h (B). Cells were then fixed and observed with confocal microscopy. The right panels show the enlarged images of the phagosomes shown at left. Scale bar, 10 μm (left panel), 3 μm (right panel). (C) The proportion of Rab7-positive phagosomes containing *M.tb* (MTB) and *S. aureus* (SA) at 30 min and 6 h postinfection. (D) The proportion of Rab7-positive phagosomes containing live (Live) and heat-inactived (Dead) *M.tb* at 6 h postinfection. Data represent the average of three independent experiments in which more than 200 phagosomes were counted for each condition in (C) and (D). $^{*}P < 0.05$. N.S., no significance. (E) Raw264.7 cells expressing EGFP-Rab7 were infected with *M.tb* expressing DsRed and analyzed by 4D microscopy. The upper and lower panels show fluorescent images of the same Raw264.7 cell expressing EGFP-Rab7 (green) with or without fluorescent images of *M.tb* (red), respectively, at the indicated times after infection. Arrow indicates *M.tb* phagosome. Scale bar, 10 μm.

We investigated the dynamics of EGFP-Rab7 localization on *M.tb* phagosomes by live 4D confocal microscopy (Fig. 1E and Movie S1). At 30 min postinfection, Rab7 was clearly present on the *M.tb* phagosome. The outline of the Rab7 signal surrounding the phagosome began to fade at 95 min and disappeared completely at 125 min. At 150 min postinfection, Rab7 was still absent from the phagosome. These results suggest that Rab7 started to localize on the majority of *M.tb* phagosome immediately after infection, but viable *M.tb* subsequently caused the dissociation of Rab7 from the phagosome.

We applied immunoelectron microscopy to investigate Rab7 localization on *M.tb* phagosomes. Macrophages expressing EGFP-Rab7 were infected with *M.tb* for 30 min or 6 h, fixed and processed for immunoelectron microscopy using anti-GFP antibody. Gold particles forming clusters were associated with *M.tb* phagosome membranes at 30 min, but not at 6 h postinfection (Fig. 2A and B). Quantitative analysis revealed that about 80% of *M.tb* phagosomes is associated with gold particles forming clusters at 30 min and that the number of gold particles associated with *M.tb* phagosomes was remarkably decreased at 6 h (Fig. 2C). These results suggest that *M.tb* phagosomes acquire Rab7 molecules by the association with Rab7-containing vesicles immediately after infection, and that this association is canceled at the later stage of infection.

To confirm biochemically that Rab7 is transiently recruited to and then dissociated from *M.tb* phagosomes, we conducted immunoblotting analysis to detect Rab7 in isolated mycobacterial phagosomal fractions. Raw264.7 macrophages were allowed to phagocytose microbeads or infected with *M.tb* for 30 min or 6 h, and the phagosomal fractions were isolated as previously reported [4,15]. We checked the purity of phagosomes by thin-section electron microscopy and immunoblotting analysis for cytochrome C, and found that few organelles and materials had contaminated in both phagosomal fractions (Supplemental Fig. 1). As shown in Fig. 3, the amount of Rab7 on *M.tb* phagosomes at 6 h postinfection decreased significantly to 19 ± 7% (mean ± standard deviation,

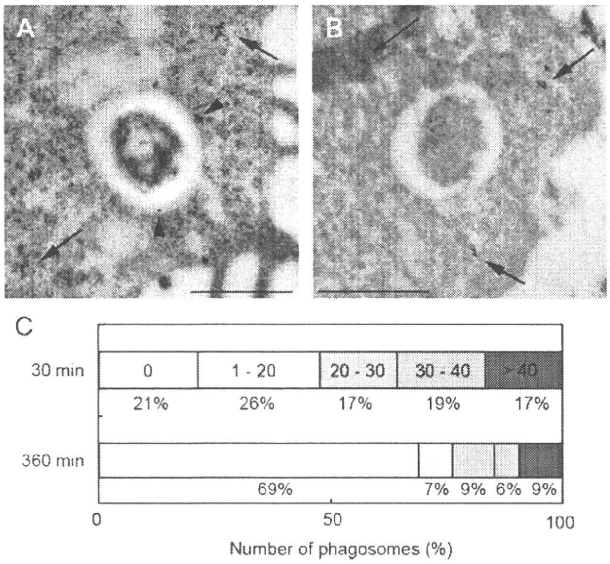

Fig. 2. Immunoelectron microscopic analysis of Rab7 localization on *M.tb* phagosomes. (A, B) Immunoelectron microscopic images of *M.tb*-infected macrophages. Raw264.7 macrophages expressing EGFP-Rab7 were infected with *M.tb* for 30 min (A) or 6 h (B) and processed for immunoelectron microscopy. Thin sections were stained with anti-GFP antibody followed by 10-nm gold-particle-conjugated secondary antibody. Arrow and arrowhead indicate gold particles forming clusters in the cytoplasmic region and on the phagosome, respectively. Scale bar, 0.5 μm. (C) Distribution of Rab7-gold particles associated with *M.tb* phagosomes. The number of gold particles on each *M.tb* phagosome in EGFP-Rab7-positive macrophages was counted at 30 min ($n = 52$ phagosomes) or 6 h ($n = 56$ phagosomes) postinfection, and the number per area (μm^2) of each phagosome was calculated. The distribution of the number of gold particles associated with the phagosome is indicated in the bar. The percentages of the different populations are shown at each time point.

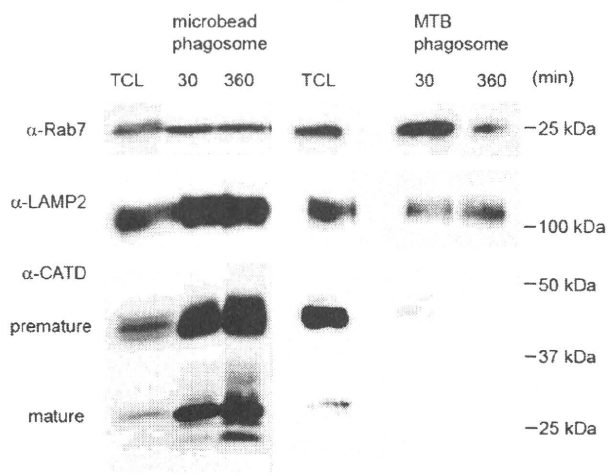

Fig. 3. Rab7 localization in isolated *M.tb* phagosomal fractions. Immunoblotting analysis of microbead and *M.tb* (MTB) phagosomal fractions with antibodies to Rab7, LAMP-2, and cathepsin D (CATD) is shown. Total cell lysates from Raw264.7 cells (TCL) and phagosomal fractions of microbead or *M.tb* were subjected to SDS–PAGE, followed by immunoblotting using indicated antibodies.

$n = 3$, $P < 0.05$) of that at 30 min, whereas the amounts on microbead phagosomes at 30 min and 6 h were nearly the same. These results are in line with those obtained by immunofluorescence and immunoelectron microscopic analyses and support the idea that Rab7 is transiently recruited to and then dissociated from *M.tb* phagosomes.

Localization of the constitutively active form of Rab7 on M.tb phagosome

It seems most likely that the dissociation of Rab7 from *M.tb* phagosomes is caused by *M.tb*-mediated conversion of its form from the GTP-bound type to the GDP-bound one. To investigate the mechanism by which Rab7 is released from *M.tb* phagosomes after transient recruitment, we employed the constitutive-active Rab7 mutant Rab7Q67L which lacks GTPase activity [18]. EGFP-fused Rab7Q67L localized on the majority of *M.tb* phagosomes at 30 min postinfection, and were dissociated from phagosomes at 6 h (data not shown), just as for the wild type of Rab7 (Fig. 1). These results suggest that the GTPase activity of Rab7 is not required for the dissociation of Rab7 from *M.tb* phagosomes. We propose two possibilities to account for the GTPase-independent dissociation of Rab7 from *M.tb* phagosomes. First, Rab7 dissociation is caused by the inactivation of the tethering and/or docking molecules of Rab7 to *M.tb* phagosome, which leads to the increase of Rab7 efflux from the phagosome. Second, vesicles containing Rab7 are transiently associated with and then dissociated from *M.tb* phagosomes at the early and late stages of infection, respectively, as shown by immunoelectron microscopy (Fig. 2).

Localization of lysosomal proteins on M.tb phagosome

To further understand the effect of Rab7 dissociation from the phagosome, we examined that lysosomal marker proteins depend on the function of Rab7 to localize on the phagosome (Fig. 4). We chose LAMP-2 and cathepsin D that have been shown to reside on microbead phagosome [19] as the lysosomal markers. Raw264.7 macrophages simultaneously transfected with two plasmids encoding EGFP and a dominant-negative form of Rab7, Rab7T22N, were allowed to phagocytose microbeads for 2 h and then stained with anti-LAMP-2 or anti-cathepsin D antibodies. In the wild type Raw264.7 cells, both lysosomal markers are localized on more than 80% of microbead phagosomes at 2 h after phagocytosis (data not shown). In Raw264.7 cells expressing Rab7T22N, LAMP-2 was recruited to microbead phagosomes (Fig. 4A), while cathepsin D was not (Fig. 4B). The results indicate that LAMP-2 on the phagosome is Rab7-independent, while that of cathepsin D is Rab7-dependent.

Both LAMP-2 and cathepsin D showed limited localizations on mycobacterial phagosomes in macrophages 24 h after infection and later [6]. However, the kinetics of their localization on mycobacterial phagosomes immediately after infection is not known. We therefore examined the localization of LAMP-2 and cathepsin D on *M.tb* phagosomes by immunofluorescence microscopy (Fig. 4). LAMP-2 localized on about 80% and 60% of *M.tb* phagosomes at 30 min and 6 h postinfection, respectively (Fig. 4C and D). Cathepsin D localized on about 50% of phagosomes at 30 min postinfection, but its localization on *M.tb* phagosome showed a punctuated staining pattern (Fig. 4E). At 6 h postinfection, it was not present on most *M.tb* phagosomes (Fig. 4F).

Localization of LAMP-2 and cathepsin D on isolated *M.tb* phagosomes was examined by immunoblotting analysis (Fig. 3C). Both lysosomal markers were present in the microbead phagosomal fractions, as previously reported [19]. In the *M.tb* phagosomal fractions, LAMP-2 was present, but cathepsin D was absent at 30 min and 6 h postinfection. The results obtained by immunofluorescence microscopic and immunoblotting analyses suggest that LAMP-2 localizes on the major proportion of *M.tb* phagosomes and that cathepsin D associates with *M.tb* phagosome immediately after infection, but the fusion of cathepsin D with *M.tb* phagosome is inhibited.

In conclusion, we propose the following model for *M.tb*-induced inhibition of phagolysosome biogenesis based on the data pre-

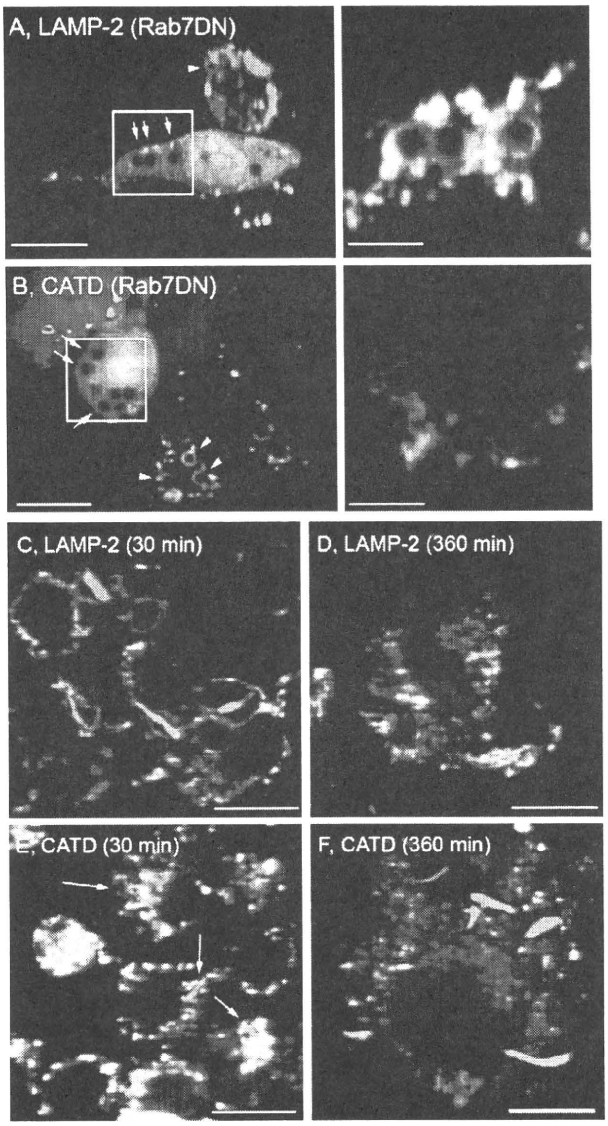

Fig. 4. Localization of lysosomal markers on *M.tb* phagosome. (A, B) Localization of LAMP-2 and cathepsin D (CATD) on microbead phagosomes in the macrophage expressing a dominant-negative form of Rab7. Raw264.7 cells transfected with two plasmids expressing EGFP and Rab7T22N, were allowed to phagocytose microbeads for 2 h. Cells were fixed, stained with anti-LAMP-2 and anti-CATD antibodies, and observed with confocal microscopy. Localization of LAMP-2 (A) and CATD (B) is shown. Arrows and arrowheads indicate the phagosomes in macrophages with and without expressing Rab7T22N, respectively. The right panels show the enlarged images of the phagosomes shown at left. Scale bar, 10 μm (left), 3 μm (right). (C–F) Localization of LAMP-2 and cathepsin D on *M.tb* phagosomes. Raw264.7 cells were infected with *M.tb* expressing DsRed for 30 min (C, E) or 6 h (D, F). Infected cells were fixed, stained with anti-LAMP-2 and anti-CATD antibodies, and observed with confocal microscopy. Localization of LAMP-2 (C, D) and CATD (E, F) is shown. Scale bar, 10 μm.

sented in this study. Early *M.tb* phagosomes can potentially fuse with late endosomes and lysosomes. However, viable *M.tb* has the ability to release Rab7 from the phagosome, resulting in the inhibition of the fusion with late endosomal and lysosomal vesicles. *M.tb* phagosomes are associated with LAMPs derived from the plasma membrane and the Golgi complex [20]. Alternatively, LAMPs are derived from the endocytic vesicles, which can fuse with the phagosome in the Rab7-independent manner. Vesicles containing cathepsin D is associated with *M.tb* phagosomes immediately after infection, but the fusion is inhibited by the uncharacterized mechanism. At the later infection, cathepsin D is not associated with the phagosomes, because dissociation of Rab7 causes the inhibition of fusion of *M.tb* phagosome with cathepsin D. Rab7 dissociation from the *M.tb* phagosome causes the blocking of subsequent phagosome maturation and phagolysosome biogenesis.

Acknowledgments

We thank Drs. Toshi Nagata and Masato Uchijima of Hamamatsu University School of Medicine for their helpful discussion. *M. tuberculosis* H37Rv was kindly provided by Dr. Isamu Sugawara of Research Institute of Tuberculosis in Tokyo. This work was supported by Grants-in-Aid for Scientific Research and COE Research from the Ministry of Education, Culture, Sports, Science and Technology of Japan; by Health and Labour Science Research Grants for Research into Emerging and Reemerging Infectious Diseases from the Ministry of Health, Labour and Welfare of Japan; and by the United States-Japan Cooperative Medical Science Committee.

Appendix A. Supplementary data

Supplementary data associated with this article can be found, in the online version, at doi:10.1016/j.bbrc.2009.06.152.

References

[1] O.V. Vieira, R.J. Botelho, S. Grinstein, Phagosome maturation: aging gracefully, Biochem. J. 366 (2002) 689–704.
[2] O.V. Vieira, R.J. Botelho, L. Rameh, S.M. Brachmann, T. Matsuo, H.W. Davidson, A. Schreiber, J.M. Backer, L.C. Cantley, S. Grinstein, Distinct roles of class I and class III phosphatidylinositol 3-kinases in phagosome formation and maturation, J. Cell Biol. 155 (2001) 19–25.
[3] O.V. Vieira, C. Bucci, R.E. Harrison, W.S. Trimble, L. Lanzetti, J. Gruenberg, A.D. Schreiber, P.D. Stahl, S. Grinstein, Modulation of Rab5 and Rab7 recruitment to phagosomes by phosphatidylinositol 3-kinase, Mol. Cell. Biol. 23 (2003) 2501–2514.
[4] M. Desjardins, L.A. Huber, R.G. Parton, G. Griffiths, Biogenesis of phagolysosomes proceeds through a sequential series of interactions with the endocytic apparatus, J. Cell Biol. 124 (1994) 677–688.
[5] J.A. Armstrong, P.D. Hart, Response of cultured macrophages to *Mycobacterium tuberculosis*, with observations on fusion of lysosomes with phagosomes, J. Exp. Med. 134 (1971) 713–740.
[6] D.L. Clemens, M.A. Horwitz, Characterization of the *Mycobacterium tuberculosis* phagosome and evidence that phagosomal maturation is inhibited, J. Exp. Med. 181 (1995) 257–270.
[7] J. Rink, E. Ghigo, Y. Kalaidzidis, M. Zerial, Rab conversion as a mechanism of progression from early to late endosomes, Cell 122 (2005) 735–749.
[8] I. Vergne, J. Chua, S.B. Singh, V. Deretic, Cell biology of mycobacterium tuberculosis phagosome, Annu. Rev. Cell Dev. Biol. 20 (2004) 367–394.
[9] L.E. Via, D. Deretic, R.J. Ulmer, N.S. Hibler, L.A. Huber, V. Deretic, Arrest of mycobacterial phagosome maturation is caused by a block in vesicle fusion between stages controlled by rab5 and rab7, J. Biol. Chem. 272 (1997) 13326–13331.
[10] V.A. Kelley, J.S. Schorey, *Mycobacterium*'s arrest of phagosome maturation in macrophages requires Rab5 activity and accessibility to iron, Mol. Biol. Cell 14 (2003) 3366–3377.
[11] N. van der Wel, D. Hava, D. Houben, D. Fluitsma, M. van Zon, J. Pierson, M. Brenner, P.J. Peters, *M. Tuberculosis* and *M. leprae* translocate from the phagolysosome to the cytosol in myeloid cells, Cell 129 (2007) 1287–1298.
[12] K. Aoki, S. Matsumoto, Y. Hirayama, T. Wada, Y. Ozeki, M. Niki, P. Domenech, K. Umemori, S. Yamamoto, A. Mineda, M. Matsumoto, K. Kobayashi, Extracellular mycobacterial DNA-binding protein 1 participates in mycobacterium-lung epithelial cell interaction through hyaluronic acid, J. Biol. Chem. 279 (2004) 39798–39806.
[13] C. Bucci, P. Thomsen, P. Nicoziani, J. McCarthy, B. van Deurs, Rab7: a key to lysosome biogenesis, Mol. Biol. Cell 11 (2000) 467–480.
[14] J. Chua, V. Deretic, *Mycobacterium tuberculosis* reprograms waves of phosphatidylinositol 3-phosphate on phagosomal organelles, J. Biol. Chem. 279 (2004) 36982–36992.
[15] W.L. Beatty, E.R. Rhoades, D.K. Hsu, F.T. Liu, D.G. Russell, Association of a macrophage galactoside-binding protein with *Mycobacterium*-containing phagosomes, Cell. Microbiol. 4 (2002) 167–176.
[16] D.L. Clemens, B.Y. Lee, M.A. Horwitz, *Mycobacterium tuberculosis* and *Legionella pneumophila* phagosomes exhibit arrested maturation despite acquisition of Rab7, Infect. Immun. 68 (2000) 5154–5166.

[17] J. Sun, A.E. Deghmane, H. Soualhine, T. Hong, C. Bucci, A. Solodkin, Z. Hmama, *Mycobacterium bovis* BCG disrupts the interaction of Rab7 with RILP contributing to inhibition of phagosome maturation, J. Leukoc. Biol. 82 (2007) 1437–1445.
[18] S. Meresse, J.P. Gorvel, P. Chavrier, The rab7 GTPase resides on a vesicular compartment connected to lysosomes, J. Cell Sci. 108 (Pt 11) (1995) 3349–3358.
[19] J. Garin, R. Diez, S. Kieffer, J.F. Dermine, S. Duclos, E. Gagnon, R. Sadoul, C. Rondeau, M. Desjardins, The phagosome proteome: insight into phagosome functions, J. Cell Biol. 152 (2001) 165–180.
[20] S. Obermuller, C. Kiecke, K. von Figura, S. Honing, The tyrosine motifs of Lamp 1 and LAP determine their direct and indirect targetting to lysosomes, J. Cell Sci. 115 (2002) 185–194.

International Journal of Systematic and Evolutionary Microbiology (2009), **59**, 1336–1341 DOI 10.1099/ijs.0.000760-0

Mycobacterium kyorinense sp. nov., a novel, slow-growing species, related to *Mycobacterium celatum*, isolated from human clinical specimens

Mitsuhiro Okazaki,[1] Kiyofumi Ohkusu,[2] Hiroyuki Hata,[2] Hiroaki Ohnishi,[1] Keiko Sugahara,[3] Chizuko Kawamura,[4] Nagatoshi Fujiwara,[5] Sohkichi Matsumoto,[5] Yukiko Nishiuchi,[6] Kouichi Toyoda,[7] Hajime Saito,[8] Shota Yonetani,[1] Yoko Fukugawa,[1] Masayuki Yamamoto,[9] Hiroo Wada,[9] Akiko Sejimo,[3] Akio Ebina,[4] Hajime Goto,[9] Takayuki Ezaki[2] and Takashi Watanabe[1]

Correspondence
Hiroaki Ohnishi
onishi@ks.kyorin-u.ac.jp

[1]Department of Laboratory Medicine, Kyorin University School of Medicine, 6-20-2 Shinkawa, Mitaka-shi, Tokyo 181-8611, Japan

[2]Department of Microbiology, Regeneration and Advanced Medical Science, Gifu University Graduate School of Medicine, Gifu, 1-1 Yanagido, Gifu City, Gifu 501-1194, Japan

[3]National Hospital Organization Tokyo National Hospital, 3-1-1 Takeoka, Kiyose-shi, Tokyo 204-0023, Japan

[4]Central Laboratory, Aomori Prefectural Hospital, 2-1-1 Higashizoudou, Aomori-shi, Aomori 030-8553, Japan

[5]Department of Host Defense, Osaka City University, Graduate School of Medicine, 1-4-3 Asahi-machi, Abeno-ku, Osaka-shi 545-8585, Japan

[6]Toneyama Institute for Tuberculosis Research, Osaka City University Medical School, Osaka, Japan

[7]Kyokuto Pharmaceutical Industrial Co. Ltd, 7-8, Nihonbashi-kobunachou, Chuuou-ku, Tokyo, 103-0024, Japan

[8]Hiroshima Environment & Health Association, Health Science Center, 9-1 Hirosekita-machi, Naka-ku, Hiroshima 730-8631, Japan

[9]Department of Respiratory Medicine, Kyorin University School of Medicine, 6-20-2 Shinkawa, Mitaka-shi, Tokyo 181-8611, Japan

A novel, non-pigmented, slow-growing mycobacterium was identified on the basis of biochemical and nucleic acid analyses, as well as growth characteristics. Three isolates were cultured from clinical samples (two from sputum and one from pus in lymph nodes) obtained from three immunocompetent patients with infections. Bacterial growth occurred at 28–42 °C on Middlebrook 7H11-OADC agar. The isolates showed negative results for Tween hydrolysis, nitrate reductase, semiquantitative catalase, urease activity, 3 day arylsulfatase activity, pyrazinamidase, tellurite reduction and niacin accumulation tests, but positive results for 14 day arylsulfatase activity and heat-stable catalase tests. The isolates contained α-, keto-, and dicarboxymycolates in their cell walls. Sequence analysis revealed that all isolates had identical, unique 16S rRNA sequences. Phylogenetic analysis of the 16S rRNA, *rpoB*, *hsp65* and *sodA* gene sequences confirmed that these isolates are unique but closely related to *Mycobacterium celatum*. DNA–DNA hybridization of the isolates demonstrated less than 50 % reassociation with *M. celatum* and *Mycobacterium branderi*. On the basis of these findings, a novel species designated *Mycobacterium kyorinense* sp. nov. is proposed. The type strain is KUM 060204^T (=JCM 15038^T=DSM 45166^T).

The GenBank/EMBL/DDBJ accession numbers for the 16S rRNA, *hsp65*, *proB* and *sodA* gene sequences of strains KUM 060204^T, NTH 512-121 and AHM 060905 are, respectively: AB370111, AB370169 and AB370170 (16S rRNA); AB370171, AB370176, and AB370177 (*hsp65*); AB370178, AB370182, and AB370183 (*rpoB*); AB370184, AB370188, and AB370189 (*sodA*).

INTRODUCTION

The advent of new molecular techniques has evoked great interest in the identification and classification of non-tuberculous mycobacteria that cause infectious diseases in mammals. Currently, there are more than 100 species of non-tuberculous mycobacteria, of which approximately 60 are considered to be potential pathogens (Brown-Elliott & Wallace, 2005). Among the non-tuberculous mycobacteria, *Mycobacterium celatum* was first described by Butler *et al.* (1993). It has unique species-specific 16S rRNA and superoxide dismutase sequences, resembling those of *Mycobacterium xenopi*, but is biochemically indistinguishable from the *Mycobacterium avium* complex (Butler *et al.*, 1993). Sequencing analysis of the 16S rRNA gene in additional *M. celatum* strains revealed the existence of a new subtype, which is distinct from but very similar to the two previously reported subtypes (types 1 and 2) (Butler *et al.*, 1993). Furthermore, *Mycobacterium branderi* was described as a novel species in 1995, and analysis of its 16S rRNA sequence has confirmed the close phylogenetic relationship of this organism to *M. celatum* (Koukila-Kahkola *et al.*, 1995).

In this study, slow-growing mycobacteria with a close phylogenetic relationship to *M. celatum* were isolated from clinical specimens from three Japanese patients with infections. Biochemical tests and genotypic analyses revealed that these isolates belong to the same novel species of the genus *Mycobacterium* for which the name *Mycobacterium kyorinense* is proposed.

METHODS

Bacterial strains. Strain KUM 060204^T was isolated from the sputum of a 62-year-old Japanese man with pneumonia at Kyorin University Hospital in Mitaka City, Tokyo, Japan. Three more isolates were obtained from the sputa of the same patient at different time points, but later analyses revealed that all four isolates were identical. Therefore, these four isolates were referred to as a single strain, KUM 060204^T. Strain NTH 512-121 was isolated from the sputum of a 70-year-old Japanese man with pneumonia at the National Hospital Organization Tokyo National Hospital in Kiyose City, Tokyo, Japan. Strain AHM 060905 was isolated from pus from cervical lymph nodes of a 64-year-old Japanese woman with non-tuberculous mycobacterial lymphadenitis at Aomori Prefectural Hospital in Aomori City, Aomori, Japan. None of these three patients suffered underlying immunocompromising disease. Since strains KUM 060204^T and AHM 060905 fulfil the criteria for infections of clinical significance (Medical Section of the American Lung Association, 1997), these two strains were considered to be clinically relevant in immunocompetent patients. *M. celatum* ATCC 51131^T, *M. branderi* ATCC 51789^T and *M. branderi* ATCC 51788 were purchased from ATCC and used as standard strains.

Phenotypic properties. Bacterial morphology and acid–alcohol-fastness were determined by Ziehl-Neelsen staining as described by Chapin (2007). Colony morphology, pigmentation, and the ability of the isolates to grow at various temperatures (25, 28, 30, 35 and 42 °C) were observed on Middlebrook 7H11-OADC agar (Nippon Becton Dickinson) and 1 % Ogawa egg agar (Kyokuto Pharmaceutical Industrial Co. Ltd). The following biochemical tests were performed as described by Kent & Kubica (1985): Tween hydrolysis, nitrate reductase, pyrazinamidase, tellurite reduction, urease activity, niacin accumulation, arylsulfatase activity (3- and 14-day), semiquantitative catalase and heat-stable catalase tests (68 °C).

Antimicrobial susceptibility testing. MICs for amikacin, clarithromycin, ethambutol, isoniazid, kanamycin, levofloxacin, rifampicin and streptomycin were determined based on the broth microdilution method with Broth MIC NTM (Kyokuto Pharmaceutical Industrial Co. Ltd) as described in monograph M24-A of the National Committee on Clinical Laboratory Standards, now CLSI (NCCLS, 2003).

Mycolic acid analysis by thin-layer chromatography (TLC). Mycolic acid analyses were performed using Silica gel TLC (Uniplate, 20 × 20 cm, 250 μm; Analtech) and matrix-assisted laser desorption/ionization time-of-flight mass spectrometry (MALDI-TOF MS) with an Ultraflex II (Bruker Daltonics) as described previously (Masaki *et al.*, 2006) with some modifications. *Mycobacterium tuberculosis* H37Rv ATCC 27294^T, *M. avium* ATCC 25291^T and *Mycobacterium intracellulare* ATCC 13950^T were used as controls.

Sequence determination and phylogenetic analysis. DNA was prepared after mechanical disruption of bacterial cells and subjected to sequence analysis of the 16S rRNA, *hsp65*, *rpoB* and *sodA* genes using methods as described by Kirschner *et al.* (1993), Telenti *et al.* (1993), Boor *et al.* (1995) and Domenech *et al.* (1997) with some modifications. Phylogenetic trees with bootstrap values were generated using the CLUSTAL W program (www.clustal.org) and displayed using TREEVIEW as described by Li *et al.* (2004). Phylogenetic analyses were also performed using the neighbour-joining method with Kimura's two-parameter distance correction model with 100 bootstrap replications in the MEGA version 2.1 software package. Homology searching with the 16S rRNA, *hsp65*, *rpoB* and *sodA* gene sequences was performed against sequences registered in GenBank/EMBL/DDBJ using BLAST.

DNA–DNA hybridization. Quantitative microplate DNA–DNA hybridization for selected strains was carried out under optimal conditions as described by Ezaki *et al.* (1988, 1989).

RESULTS AND DISCUSSION

The three isolates examined were acid–alcohol-fast, non-motile, non-spore-forming bacilli. Mature colonies of all isolates developed in 4 weeks on Middlebrook 7H11-OADC agar. Growth was observed at temperatures in the range 28–42 °C, with optimal growth obtained at 30–35 °C. No growth was observed at 25 °C. Colonies were smooth and initially transparent, but became creamy white on prolonged culture.

All three isolates were negative for Tween hydrolysis, nitrate reductase, semiquantitative catalase, urease activity, 3-day arylsulfatase activity, pyrazinamidase, tellurite reduction and niacin accumulation, but positive for 14-day arylsulfatase activity and heat-stable catalase (Table 1). All isolates were distinguishable from *M. celatum* and *M. branderi* by a lack of growth at 25 °C and a negative pyrazinamidase test. They were also distinguishable from *M. celatum* by a negative result for 3-day arylsulfatase activity and the tellurite reduction test. The three isolates were also distinct from *Mycobacterium cookii* by their ability to grow at 45 °C and a lack of growth at 25 °C, absence of pigment production in the dark, and a negative semiquantitative catalase test. They were also distinct from

Table 1. Growth characteristics of strain KUM 060204^T in comparison with the closely related species *M. celatum* and *M. branderi*

+, Positive; –, negative; ND, not done.

Characteristic	KUM 060204^T	*M. celatum**	*M. branderi**
Growth temperature (°C)			
25	–	+	+
28	+	+	ND
30	+	+ (31 °C)	ND
35	+	ND	ND
42	+	+ (45 °C)	+ (45 °C)
Heat-stable catalase (68 °C)	+	+	–
Arylsulfatase activity			
3 days	–	+	–
14 days	+	+	+
Pyrazinamidase	–	+	+
Tellurite reduction	–	+	ND

*Data taken from Butler *et al.* (1993), Koukila-Kahkola *et al.* (1995) and Vincent & Gutierres (2007).

M. xenopi by the lack of pigment production in the dark (Koukila-Kahkola *et al.*, 1995).

Using antimicrobial susceptibility tests, all isolates were shown to be susceptible to clarithromycin and ethambutol, but resistant to isoniazid and rifampicin. Amikacin, kanamycin, levofloxacin and streptomycin showed low MIC values against all three isolates (Table 2).

Mycolic acid analyses of the three isolates by TLC produced identical multispot patterns composed of α- (C82-86)-, keto (C84-89)- and dicarboxy- (C64-69) mycolates. The length of the carbon chain of each mycolic acid methyl ester was assigned by the mass number and proposed structures as summarized in Table 3. The mycolic acids contained predominantly one or two cyclopropane rings. This pattern of mycolic acid subclasses is characteristic for the *Mycobacterium avium* complex, and is also seen in *M. celatum* and *M. branderi*, suggesting that the new isolates are closely related to these *Mycobacterium* species (Fig. 1) (Butler *et al.*, 1993; Brander *et al.*, 1992).

Table 2. Susceptibility of the three isolates to various antibiotics

Antibiotic	MIC (μg ml^{-1})		
	KUM 060204^T	NTH 512-121	AHM 060905
Amikacin	<0.5	<0.5	<0.5
Clarithromycin	<0.03	<0.03	<0.03
Ethambutol	4	2	4
Isoniazid	16	32	16
Kanamycin	0.5	0.25	1
Levofloxacin	0.125	<0.03	0.125
Rifampicin	32	>32	>32
Streptomycin	0.25	0.25	0.25

The sequence of the 16S rRNA gene was identical in all strains, but was different from all other available 16S rRNA sequences. The sequences of the *hsp65*, *rpoB* and *sodA* genes were also identical in the three isolates. It was assumed that these three isolates belong to the same species, and strain KUM 060204^T was used as a representative strain for genotypic analyses thereafter.

Sequence analysis revealed that the 16S rRNA gene sequence of the newly identified mycobacterium was closest to that of *M. celatum* ATCC 51130 (type 2) with 18 base mismatches out of 1469 bp (98.8 % identity). It was also highly similar to that of *M. celatum* NCTC 12882 (type 3) with 25 base mismatches out of 1476 bp (98.3 %), *M. celatum* ATCC 51131^T (type 1) with 27 base mismatches out of 1450 bp (98.1 %), *M. branderi* ATCC 51789^T with 32 base mismatches out of 1476 bp (97.8 %) and *M. cookii* ATCC 49103^T with 41 base mismatches out of 1477 bp (97.2 %). A phylogenetic tree was created based on the 16S rRNA gene sequences, incorporating all previously described species of slow-growing mycobacteria. Phylogenetic analysis revealed that strain KUM 060204^T is adjacent to the type strains of *M. celatum* (ATCC 51131^T), *M. branderi* (ATCC 51789^T) and *M. cookii* (ATCC 49103^T) (Fig. 2a).

The *hsp65* gene sequence of strain KUM 060204^T was identical to that of *M. celatum* ATCC 51130 (392/392, 100 %) and highly similar to those of *M. branderi* ATCC 51789^T and *M. celatum* ATCC 51131^T (98.8 and 98.1 %, respectively). A phylogenetic tree based on the *hsp65* sequences is shown in Fig. 2(b). Phylogenetic analysis of the *hsp65* gene gave consistent results, i.e. strain KUM 060204^T is located adjacent to the type strains of *M. branderi* (ATCC 51789^T) and *M. celatum* (ATCC 51131^T).

The sequence of the *rpoB* gene of strain KUM 060204^T was identical to that of *M. celatum* ATCC 51130 (306/306, 100 %) and highly similar to that of *M. branderi* ATCC 51789^T (96.7 %). It showed further differences from those of *M. celatum* ATCC 51131^T and *M. cookii* ATCC 49103^T (94.1 and 92.7 %, respectively). Strain KUM 060204^T clustered adjacent to *M. branderi* ATCC 51789^T and *M. celatum* ATCC 51131^T (Fig. 2c) in a phylogenetic tree based on *rpoB* sequences.

The *sodA* gene of strain KUM 060204^T was almost identical to that of *M. celatum* ATCC 51130 (411/413, 99.5 %) and highly similar to that of *M. celatum* ATCC 51131^T (96.6 %). It showed further differences from those of *M. branderi* ATCC 51789^T and *M. xenopi* ATCC 19250^T (90.1 and 86.4 %, respectively) (Fig. 2d).

Given the close relationship of strain KUM 060204^T to *M. celatum* and *M. branderi*, a DNA–DNA hybridization study was performed for these strains under optimal conditions (Table 4). Strain KUM 060204^T exhibited DNA similarity values below the suggested species threshold (70 %) to its

Table 3. The relationship between molecular species and mass numbers in each mycolic acid subclass

Underlining indicates a major component.

Strain		α-MA	Keto-MA	Dicarboxy-MA
KUM 060204^T	Mass number [M+Na]+	1230, 1258, 1286	1274, 1302, 1316, 1344	1024, 1038, 1052, 1066, 1080, 1094
	Molecular species (carbon-chain length)	82:2, 84:2, 86:2	84:1, 86:1, 87:1, 89:1	64:1, 65:1, 66:1, 67:1, 68:1, 69:1
NTH 512-121	Mass number [M+Na]+	1230, 1258, 1286	1302, 1316, 1344	1024, 1038, 1052, 1066, 1080, 1094
	Molecular species (carbon-chain length)	82:2, 84:2, 86:2	86:1, 87:1, 89:1	64:1, 65:1, 66:1, 67:1, 68:1, 69:1
AHM 060905	Mass number [M+Na]+	1230, 1258, 1286	1302, 1316, 1344	1024, 1038, 1052, 1066, 1080, 1094
	Molecular species (carbon-chain length)	82:2, 84:2, 86:2	86:1, 87:1, 89:1	64:1, 65:1, 66:1, 67:1, 68:1, 69:1

phylogenetic neighbours *M. celatum* ATCC 51131^T, *M. branderi* ATCC 51789^T and *M. branderi* ATCC 51788 (similarity 49.9, 44.5 and 41.5 %, respectively). These results provide further evidence for the genetic diversity between this strain and closely related species, indicating that this isolate comprises a new mycobacterial species.

Based on the genotypic and phenotypic data described above, it was concluded that strain KUM 060204^T represents a novel *Mycobacterium* species for which we propose the name *Mycobacterium kyorinense* sp. nov. Two other strains, NTH 512-121 and AHM 060905, were assumed to belong to the same species as strain KUM 060204^T based on sequence identity. Considering that strains KUM 060204^T and AHM 060905 fulfil the criteria for clinical significance, this newly identified *Mycobacterium* is considered to be a potential pathogen for infection in humans.

Description of *Mycobacterium kyorinense* sp. nov.

Mycobacterium kyorinense (kyo.rin.en'se. N.L. neut. adj. *kyorinense* of Kyorin, referring to the Kyorin University Hospital where the first strain was isolated).

Long, rod-shaped cells (approx. 3 × 0.3 μm); acid–alcohol-fast. Growth requires >4 weeks at 28–42 °C. No growth occurs at 25 °C. Colony diameters are 1–2 mm on Middlebrook 7H11-OADC agar. Colonies on 1 % Ogawa egg agar are smooth and raised with round or lobate regular margins, and non-chromogenic. Negative for Tween hydrolysis, nitrate reductase, semiquantitative catalase, urease activity, 3-day arylsulfatase activity, pyrazinamidase, tellurite reduction and niacin accumulation; positive for 14-day arylsulfatase activity and heat-stable catalase tests. Susceptible to clarithromycin and ethambu-

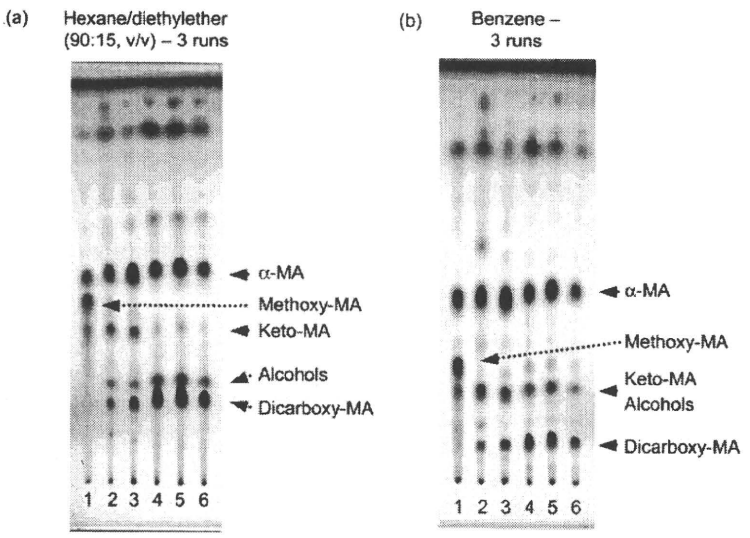

Fig. 1. TLC patterns of mycolic acid methyl esters. (a) Plate developed three times with hexane/diethylether. (b) Plate developed three times with benzene. Lanes: 1, *M. tuberculosis* H37Rv ATCC 27294^T; 2, *M. avium* ATCC 25291^T; 3, *M. intracellulare* ATCC 13950^T; 4, strain KUM 060204^T; 5, strain NTH 512-121; 6, strain AHM 060905. MA, Mycolic acid.

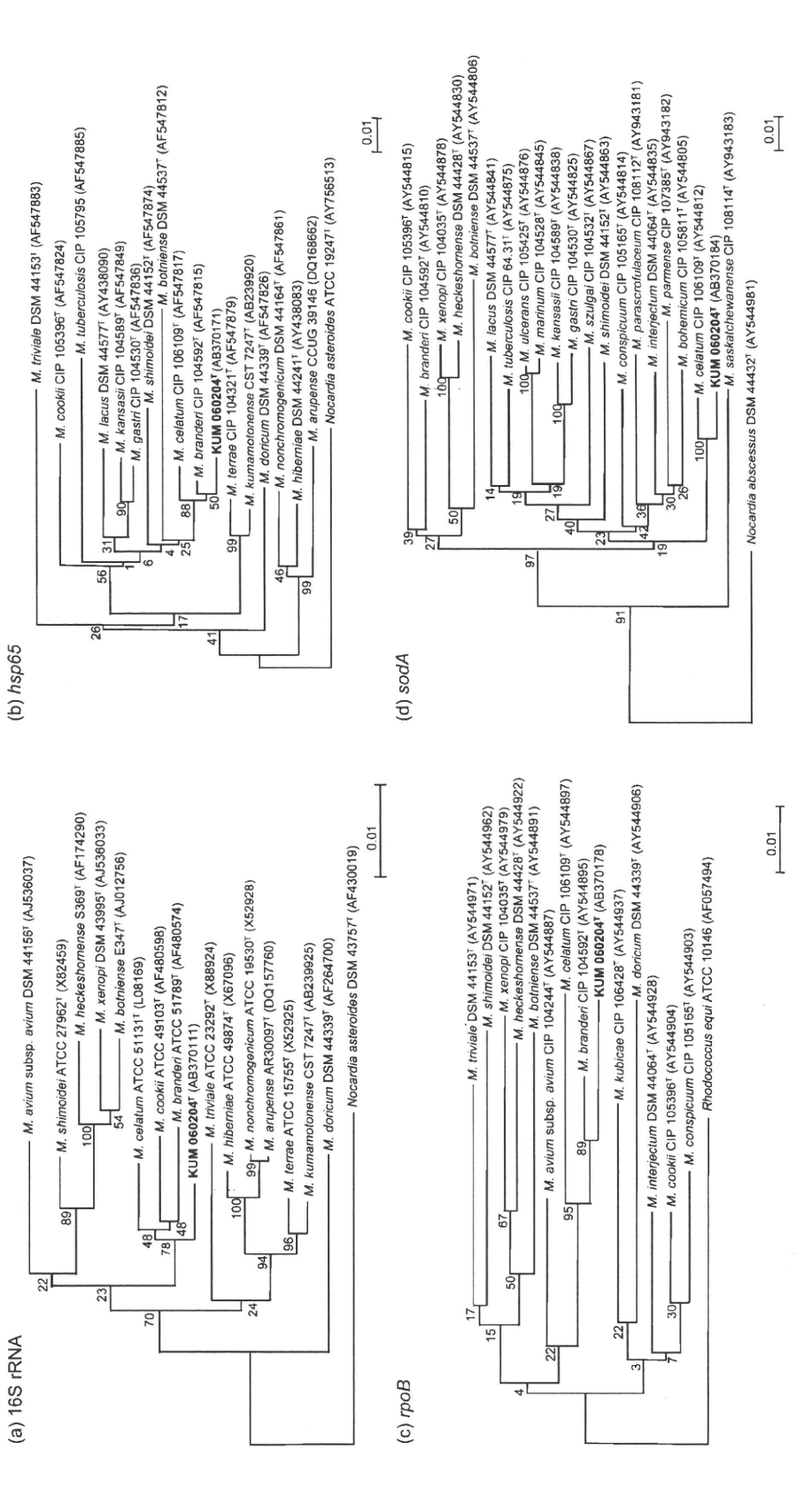

Fig. 2. Phylogenetic trees for isolate KUM 060204^T and closely related type strains of other mycobacterial species based upon comparisons of (a) 16S rRNA, (b) *hsp65*, (c) *rpoB* and (d) *sodA* gene sequences using the neighbour-joining method. The trees were rooted using the sequences of *Nocardia asteroides* (16S rRNA and *hsp65*), *Rhodococcus equi* (*rpoB*) and *Nocardia abscessus* (*sodA*) as the outgroups. The scale bars represent a 1% sequence difference.

Table 4. Levels of DNA–DNA relatedness between strain KUM 060204^T and related *Mycobacterium* species

Strain	Similarity value (%) with labelled DNA from:			
	KUM 060204^T	*M. celatum* ATCC 51131^T	*M. branderi* ATCC 51789^T	*M. branderi* ATCC 51788
KUM 060204^T	100	49.1	46.0	47.6
M. celatum ATCC 51131^T	49.9	100	62.4	59.8
M. branderi ATCC 51789^T	44.5	51.3	100	100
M. branderi ATCC 51788	41.5	46.2	92.5	100

tol, but resistant to isoniazid and rifampicin. Sequence analysis of the 16S rRNA, *hsp65*, *rpoB* and *sodA* genes indicated that *M. kyorinense* is a mycobacterial species most closely related to *M. celatum* and *M. branderi*. DNA–DNA hybridization revealed that *M. kyorinense* exhibits DNA similarity values below the suggested threshold with its phylogenetic neighbours *M. celatum* ATCC 51131^T, *M. branderi* ATCC 51789^T and *M. branderi* ATCC 51788 (similarity 49.9, 44.5 and 41.5%, respectively), thus defining it as a distinct species. *M. kyorinense* was placed in the slow-growing mycobacteria group.

The type strain is KUM 060204^T (=JCM 15038^T=DSM 45166^T), isolated from sputum in a patient with pneumonia.

ACKNOWLEDGEMENTS

This work was supported by grants from the Ministry of Health, Labour and Welfare (Research on Emerging and Re-emerging Infectious Diseases, Health Sciences Research Grants) of Japan, The Japan Health Sciences Foundation, Ministry of Education Culture Sports Science and Technology, and The United States–Japan Cooperative Medical Science Program against Tuberculosis and Leprosy.

REFERENCES

Boor, K. J., Duncan, M. L. & Price, C. W. (1995). Genetic and transcriptional organization of the region encoding the beta subunit of *Bacillus subtilis* RNA polymerase. *J Biol Chem* **270**, 20329–20336.

Brander, E., Jantzen, E., Huttunen, R., Julkunen, A. & Katila, M. L. (1992). Characterization of a distinct group of slowly growing mycobacteria by biochemical tests and lipid analyses. *J Clin Microbiol* **30**, 1972–1975.

Brown-Elliott, B. & Wallace, R. J., Jr (2005). Infections caused by nontuberculous mycobacteria. In *Principles and Practice of Infectious Diseases*, vol. 2, pp. 2909–2915. Edited by G. L. Mandell, J. E. Bennett & R. Dolin. Pennsylvania: Elsevier.

Butler, W. R., O'Connor, S. P., Yakrus, M. A., Smithwick, R. W., Plikaytis, B. B., Moss, C. W., Floyd, M. M., Woodley, C. L., Kilburn, J. O. & other authors (1993). *Mycobacterium celatum* sp. nov. *Int J Syst Bacteriol* **43**, 539–548.

Chapin, K. C. (2007). Principles of stains and media. In *Manual of Clinical Microbiology*, 9th edn, pp. 182–191. Edited by P. R. Murray, E. J. Baron, M. L. Landry, J. H. Jorgensen & M. A. Pfaller. Washington, DC: American Society for Microbiology.

Domenech, P., Jimenez, M. S., Menendez, M. C., Bull, T. J., Samper, S., Manrique, A. & Garcia, M. J. (1997). *Mycobacterium mageritense* sp. nov. *Int J Syst Bacteriol* **47**, 535–540.

Ezaki, T., Hashimoto, Y., Takeuchi, N., Yamamoto, H., Liu, S. L., Miura, H., Matsui, K. & Yabuuchi, E. (1988). Simple genetic method to identify viridans group streptococci by colorimetric dot hybridization and fluorometric hybridization in microdilution wells. *J Clin Microbiol* **26**, 1708–1713.

Ezaki, T., Hashimoto, Y. & Yabuuchi, E. (1989). Fluorometric deoxyribonucleic acid–deoxyribonucleic acid hybridization in micro-dilution wells as an alternative to membrane filter hybridization in which radioisotopes are used to determine genetic relatedness among bacterial strains. *Int J Syst Evol Microbiol* **39**, 224–229.

Kent, P. T. & Kubica, G. P. (1985). *Public Health Mycobacteriology: a Guide for the Level III Laboratory.* Atlanta: US Department of Health and Human Services, Centers for Disease Control.

Kirschner, P., Springer, B., Vogel, U., Meier, A., Wrede, A., Kiekenbeck, M., Bange, F. C. & Bottger, E. C. (1993). Genotypic identification of mycobacteria by nucleic acid sequence determination: report of a 2-year experience in a clinical laboratory. *J Clin Microbiol* **31**, 2882–2889.

Koukila-Kahkola, P., Springer, B., Bottger, E. C., Paulin, L., Jantzen, E. & Katila, M. L. (1995). *Mycobacterium branderi* sp. nov., a new potential human pathogen. *Int J Syst Bacteriol* **45**, 549–553.

Li, Y., Kawamura, Y., Fujiwara, N., Naka, T., Liu, H., Huang, X., Kobayashi, K. & Ezaki, T. (2004). *Sphingomonas yabuuchiae* sp. nov. and *Brevundimonas nasdae* sp. nov., isolated from the Russian space laboratory Mir. *Int J Syst Evol Microbiol* **54**, 819–825.

Masaki, T., Ohkusu, K., Hata, H., Fujiwara, N., Iihara, H., Yamada-Noda, M., Nhung, P. P., Hayashi, M., Asano, Y. & other authors (2006). *Mycobacterium kumamotonense* sp. nov. recovered from clinical specimen and the first isolation report of *Mycobacterium arupense* in Japan: novel slowly growing, nonchromogenic clinical isolates related to *Mycobacterium terrae* complex. *Microbiol Immunol* **50**, 889–897.

Medical Section of the American Lung Association (1997). Diagnosis and treatment of disease caused by nontuberculous mycobacteria. This official statement of the American Thoracic Society was approved by the Board of Directors, March 1997. *Am J Respir Crit Care Med* **156**, S1–S25.

NCCLS (2003). *Susceptibility Testing of Mycobacteria, Nocardiae, and Other Aerobic Actinomycetes; Approved Standard.* NCCLS document M24-A. Wayne, PA: National Committee for Clinical Laboratory Standards.

Telenti, A., Marchesi, F., Balz, M., Bally, F., Bottger, E. C. & Bodmer, T. (1993). Rapid identification of mycobacteria to the species level by polymerase chain reaction and restriction enzyme analysis. *J Clin Microbiol* **31**, 175–178.

Vincent, V. & Gutierres, M. C. (2007). Mycobacterium: laboratory characteristics of slowly growing mycobacteria. In *Manual of Clinical Microbiology*, 9th edn, pp. 573–588. Edited by P. R. Murray, E. J. Baron, M. L. Landry, J. H. Jorgensen & M. A. Pfaller. Washington, DC: American Society for Microbiology.

Jpn. J. Infect. Dis., 62, 182-186, 2009

Original Article

Mycobacterium avium Complex Organisms Predominantly Colonize in the Bathtub Inlets of Patients' Bathrooms

Yukiko Nishiuchi*, Aki Tamaru[1], Seigo Kitada[2], Takahiro Taguri[2], Sohkichi Matsumoto[3], Yoshitaka Tateishi[2,3], Mamiko Yoshimura[3], Yuriko Ozeki[3], Narumi Matsumura[2], Hisashi Ogura[4], and Ryoji Maekura[2]

Toneyama Institute for Tuberculosis Research Osaka City University Medical School, Osaka 560-8552; [1]Department of Infectious Diseases, Osaka Prefectural Institute of Public Health, Osaka 537-0025; [2]National Hospital Organization Toneyama National Hospital, Osaka 560-8552; and [3]Department of Bacteriology and [4]Department of Virology, Osaka City University Graduate School of Medicine, Osaka 545-8585, Japan

(Received February 12, 2009. Accepted March 27, 2009)

SUMMARY: Medical treatment of pulmonary *Mycobacterium avium* complex (MAC) disease does not always provide curative effects and is frequently hampered by recurrence. This suggests the presence of a reservoir for MAC in the environment surrounding patients. We previously reported the recovery of MAC isolates from the residential bathrooms of outpatients. In the present study, to ascertain the colonizing sites and the possibility of an MAC reservoir in the bathrooms of patients, we tested the recovery and the genetic diversity of MAC isolates from 6 sites of specimens, including 2 additional sampling sites, inside the showerhead and the bathtub inlet, in the residential bathrooms of patients with pulmonary MAC disease. MAC isolates were recovered from 15 out of the 29 bathrooms (52%), including specimens from 14 bathtub inlets and 3 showerheads. Nearly half of these bathrooms (7/15) contained MAC strains that were identical or similar to their respective clinical isolates. Additionally, in 5 out of 15 bathrooms, polyclonal colonization was revealed by pulsed-field gel electrophoresis. The results imply that colonization of MAC organisms in the bathrooms of MAC patients occurs predominantly in the bathtub inlets, and there is thus a risk of infection and/or reinfection for patients via use of the bathtub and other sites in the bathroom.

INTRODUCTION

The incidence of pulmonary *Mycobacterium avium* complex (MAC) disease has increased over the past several decades (1-3). MAC disease occasionally leads to death even in patients without a history of lung diseases or immunodeficiency (2,4-6) and is characterized by multiple infection with genetically different strains (7,8). Although macrolide-based regimens are effective against MAC, the cure rate with these drugs is still low (56%) because patients drop out due to drug side effects, consecutive positive culture, and recurrence (2). Kobashi and Matsushima (9) reported that 41 of their 71 patients (58%) showed negative sputum cultures after successful completion of multidrug chemotherapy including a macrolide, and 16 of these 41 patients (39%) experienced recurrence. The genotyping research has demonstrated that patients with nodular bronchiectasis have multiple and/or repeated infections, and that frequent recurrence is due to reinfection with a genetically different strain or relapse with the original strain (7,8). To prevent recurrence of MAC disease, long-term treatment such as chemotherapy for 2 years (10) or 12-month treatment leading to culture-negative sputum (3) is recommended as a reasonable endpoint. The frequent recurrence and multiple infections suggest that polyclonal MAC colonization is likely to occur in the home environment surrounding patients with pulmonary MAC disease.

MAC is widely distributed both in the natural and living environment, and these environmental organisms are thought to be a source of infections (2,5). Drinking water systems are a possible source of disseminated MAC infection (11-16), which has been detected in biofilms of water distribution systems (13). In a recent study, we recovered MAC isolates from residential bathrooms but not from other sites within the residence (17). We also found that the appearance ratio in the bathrooms of patients with pulmonary MAC disease was significantly higher than that in the bathrooms of healthy volunteers ($P = 0.01$) (17). In the present study, therefore, we tried to determine the colonizing sites and to investigate the possibility of a reservoir of MAC organisms in the bathrooms of patients with MAC disease. We sampled specimens from 6 sites in the residential bathrooms of MAC-positive patients, including 2 sampling sites that were not included in our previous study: inside the showerhead and the bathtub inlet. A traditional Japanese bathtub has a water inlet below the water level, and we reasoned that biofilm produced by MAC organisms could develop inside this inlet, as well as within the showerheads. Finally, we examined the genetic diversity of the MAC isolates from specimens in the patients' bathrooms and sputa.

MATERIALS AND METHODS

Subjects and collection of samples: We collected 6 samples from the residential bathroom of each patient: 2 water samples (shower water and used bathtub water, 200 ml each), 3 scale samples (on the surface of the showerheads, inside

*Corresponding author: Mailing address: Toneyama Institute for Tuberculosis Research Osaka City University Medical School, 5-1-1 Toneyama, Toyonaka, Osaka 560-8552, Japan. Tel: +81-6-6853-5837, Fax: +81-6-6853-5839, E-mail: nishiuchi@med.osaka-cu.ac.jp

the showerhead, and inside the bathtub inlet), and 1 sample from the slime on the bathroom drain. Participants were outpatients diagnosed with pulmonary MAC disease ($n = 29$). All patients lived with their family and shared their bathroom with at least one other family member. Patients were diagnosed with pulmonary MAC disease according to the American Thoracis Society 1997 diagnostic criteria (18). Informed consent was obtained from all participants before the collection of samples. This study was approved by the Toneyama National Hospital institutional review board and complies with international guidelines for studies involving human subjects. Information regarding the bathrooms was collected by a questionnaire survey.

Culture of residential samples: The collected residential samples were cultured as described previously (17). In brief, water samples were centrifuged at 11,800 × g for 30 min at 4°C, and pellets from the shower water were suspended in 0.5 ml of phosphate buffer (PB) at pH 6.8, 200 μl of which was inoculated onto a Middlebrook 7H11-OADC agar plate containing the antibiotic mixture PANTA (7H11 PANTA plate). The pellet from the used bathtub water was treated with 3 ml of 2% sodium hydroxide solution for 10 min. After adding 6 ml of PB to this alkali-treated sample, it was centrifuged at 2,270 × g for 15 min, and resuspended in 0.5 ml of PB. The collected samples on the swabs were preincubated for 3 h at 25°C in a tryptic soy broth followed by alkali treatment, and the pellets were suspended in 1 ml of PB solution. One hundred to 200 μl of these suspensions were inoculated onto 7H11 PANTA plates at 37°C for 3 weeks. Growing colonies were examined microscopically, followed by Ziehl-Neelsen staining. The isolated acid-fast bacterial species were identified by the PCR method (19).

Genotypic analysis: Genotypic analyses were carried out using pulsed-field gel elecrophoresis (PFGE) as described previously (17). PFGE genotypic patterns were defined as follows: identical, when one case was not distinguishable from another; related, when the genotypic pattern differed by only 1-3 bands; and unrelated, when the genotypic pattern differed by 4 or more bands.

Statistical analysis: The chi-square and Mann-Whitney U-test were used for analysis. Findings of $P < 0.05$ were considered statistically significant, while those of $P < 0.1$ were considered as evidence of a statistical tendency.

RESULTS

Colonization of MAC in residential bathrooms: MAC isolates were frequently recovered from the residential bathrooms of outpatients with pulmonary MAC disease (Table 1). Twenty-nine bathrooms of patients were inspected in the present study, of which 15 and 1 were found to harbor *Mycobacterium avium* (52%) and *M. intracellulare* (3.4%), respectively. MAC isolates were recovered from 4 shower specimens in 3 bathrooms (3/29, 10%); the shower specimens were taken from the inside and surface of the showerheads, and from the shower water. MAC isolates were most frequently recovered from the scale of the bathtub inlets (14/25, 56%), though they were distributed throughout the bathroom (Table 1). In 7 specimens from bathtub inlets, more than 100 colonies of MAC were recovered from each primary isolation plate. The additional sampling sites were responsible for the increase in the recovery rate from 18% in our previous study (17) to 52% in the present study. In order to ascertain whether MAC continuously inhabits the inside of the showerheads and bathtub inlets, we took additional samples from these sites after an interval of 3 months in 2 bathrooms. MAC isolates were recovered from both sites (data not shown), indicating a long-lasting colonization of MAC at these sites.

Polyclonal MAC colonization: MAC isolates were recovered from more than 2 sampling sites in the bathrooms of 10 participants. Additionally, in some cases we obtained multiple isolates of MAC possessing a colony morphology different from that of the primary isolation plate. In order to clarify the genetic diversity of multiple MAC isolates from individual bathrooms, we analyzed the polymorphism of MAC isolates using PFGE (Fig. 1). In each of 5 bathrooms, we found multiple isolates that possessed different genotypic profiles. This demonstrated that polyclonal MAC colonization can occur within a single bathroom. In the case of patient #29 (P29), 5 MAC isolates were recovered from 3 different sampling sites, and they had 3 different PFGE profiles (Fig. 1). Interestingly, 3 MAC isolates from the bathtub inlet, each possessing a different colony morphology, also showed 3 different PFGE profiles. Similarly, unrelated genotypes of plural isolates recovered from 1 sampling site were observed in the cases of P8 and P17. These results indicate that polyclonal MAC strains are capable of growing together in the same location. In the case of P27, MAC isolates were recovered from 4 different sampling sites, and all of them had related PFGE profiles with 1-3 band differences (Fig. 1). Moreover, in the case of P9, 3 of 4 isolates which were recovered from 2 different sampling sites showed related PFGE profiles (Fig. 1). These related PFGE profiles reflect the genomic variation which may have occurred due to mutation of one of the strains.

Identical/related polymorphism between environmental and clinical isolates: To assess the relationship between the patient-derived clinical MAC isolates and the respective environmental isolates, we compared their polymorphism in

Table 1. Recovery of *M. avium* and *M. intracellulare* from residential bathrooms of outpatients with pulmonary MAC disease

	Sampling site						Total Sample (Residence)
	Surface of the shower head	Inside the shower head	Shower water	Bathtub inlet	Bathtub water	Drain	
No. of test samples	29	24	29	25	26	29	162 (29)
M. avium	1	2	1	14[1)]	7	7[2)]	32 (15)
M. intracellulare	0	0	0	0	0	1	1 (1)

Data are represented as the number of samples from which *M. avium* or *M. intracellulare* were recovered.
Numbers in parenthesis represent the number of residences.
[1)]: Over 100 colonies of *M. avium* in a primary isolation plate were recovered from 7 of 14 culture-positive samples.
[2)]: Over 100 colonies of *M. avium* in a primary isolation plate were recovereo from 2 of 7 culture-positive samples.

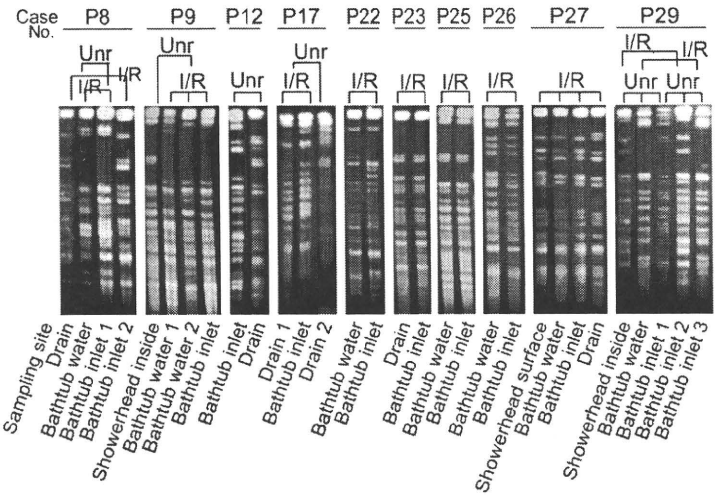

Fig. 1. Polyclonal colonization of *M. avium* complex (MAC) in residential bathrooms. Pulsed-field gel electrophoresis (PFGE) profiles of chromosomal *Xba*I digests of MAC isolates. Unr, unrelated profiles; I/R, identical or related profiles.

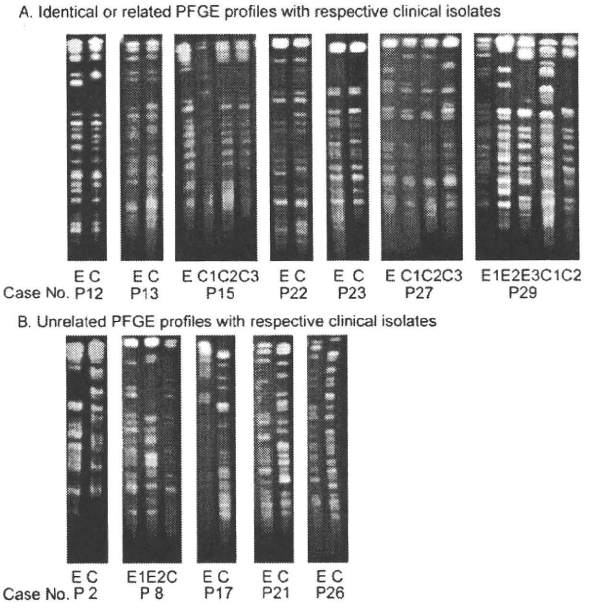

Fig. 2. Molecular typing of environmental and clinical *M. avium* complex (MAC) isolates. (A) Identical or related PFGE profiles of isolates from bathrooms with respective clinical isolates. E, environmental isolates; C, clinical isolates. C1 of P15, isolate from sputum 1 in December 2001; C2 of P15, isolate from sputum 2 in May 2003; C3 of P15, isolate from sputum 3 in January 2004; E of P27, isolate from bathtub inlet; C1 of P27, isolate from sputum 1 in December 2006; C2 of P27, isolate from sputum 2 in February 2007; C3 of P27, isolate from sputum 3 in July 2007; E1 of P29, isolates from bathtub inlet 1; E2 of P29, isolate from bathtub inlet 2; E3 of P29, isolate from bathtub inlet 3; C1 of P29, isolate from sputum 1 in June 2004; C2 of P29, isolate from sputum 2 in March 2006. (B) Unrelated PFGE profiles of isolates from bathrooms with respective clinical isolates. E1 of P8, isolate from drain; E2 of P8, isolate from bathtub inlet 1; E of P17, isolate from drain 2; E of P26, isolate from bathtub inlet.

individual cases. We recovered MAC in 15 cases, of which 11 and 1 cases were determined to contain *M. avium* isolates and *M. intracellulare* isolates, respectively, in both their environmental and clinical specimens. In the remaining 3 cases, *M. avium* isolates were recovered from the environment and *M. intracellulare* isolates were recovered from clinical specimens. Therefore, we compared the MAC genotypes in the former 12 cases. In 7 of 15 cases (47%), MAC isolates from the patients' bathrooms and their respective sputa had identical or related molecular profiles by PFGE anlysis (Fig. 2). In the other 5 cases, MAC isolates from the bathrooms possessed profiles different from those of their respective sputa (Fig. 2). These results are in agreement with our previous findings (17) that environmental isolates exhibit the identical polymorphism with their respective clinical isolates. The rate of identity obtained in the present study (47%, 7/15) is higher than that observed in the previous study (22%, 2/9) (17). We could compare the genetic diversity of retrospective sputum cultures in 3 cases. Genotypic analyses showed unrelated polymorphisms in 2 of these cases (Fig. 2, P15 and P29). The genotypes of the latent clinical strains were related to those of isolates from their respective bathrooms.

Bathtub types and bathroom maintenance: MAC bacilli appear to colonize in the bathroom preferentially over other household locations. However, no MAC isolates were recovered from half of the bathrooms examined in the present study. Therefore, to identify the risk factors for MAC colonization, we collected information regarding the type of bathtub and the method of maintaining the bathroom by a questionnaire survey. The characteristics of culture-negative versus culture-positive bathrooms are presented in Table 2. In the traditional Japanese bath, a bathtub inlet is installed inside the bathtub and below the water level. Some of the bathtub inlets are attached to the hot-water supply, while others are attached to the bath-boiler. MAC organisms are more likely to colonize in the bathtub inlet attached to the bath-boiler than in the inlet attached to the hot-water supply ($P < 0.01$, chi-square test). The bath-boiler can be classified into two types: a natural circulation type having two holes, an inlet and outlet, and a forced circulation type having one hole. In the present study, 8 participants used the natural circulation type of bath-boiler and all the bathtub inlets were found to retain MAC bacilli. In Japan, used bathtub water is sometimes reserved in the bathtub until the next day for washing clothes or to provide for a disaster such as an earthquake. MAC isolates were more frequently recovered from the samples taken from participants who were in a habit of reserving bathtub water; this relation reached the level of a tendency but was not statistically significant ($P = 0.09$, chi-square test). There was also a nonsignificant tendency for